Osmium, Rhenium, and Group 6 Derivatives of Bis(diphenylphosphino) Alkane Undecacarbonyl Triosmium

by

Shannon Leigh Henderson
B.Sc., University of British Columbia, 2004

THESIS SUBMITTED IN PARTIAL FULFILLMENT OF
THE REQUIREMENTS FOR THE DEGREE OF

MASTER OF SCIENCE

In the Department
of
Chemistry

SIMON FRASER UNIVERSITY

2007

APPROVAL

Name: Shannon Leigh Henderson

Degree: Master of Science

Title of Thesis: Osmium, Rhenium, and Group 6 Derivatives of Bis(diphenylphosphino) alkane undecacarbonyl triosmium

Examining Committee:

Chair
Dr. George R. Agnes
Professor, Department of Chemistry

Senior Supervisor
Dr. Roland K. Pomeroy
Professor, Department of Chemistry

Dr. Zuo-Guang Ye
Professor, Department of Chemistry
Interim Supervisor for Dr. Roland K. Pomeroy

Dr. Ross H. Hill
Supervisor
Professor, Department of Chemistry

Dr. Charles J. Walsby
Supervisor
Assistant Professor, Department of Chemistry

Dr. Peter D. Wilson
Internal Examiner
Associate Professor, Department of Chemistry

Date Defended/Approved: June 29, 2007

SIMON FRASER UNIVERSITY library

DECLARATION OF PARTIAL COPYRIGHT LICENCE

The author, whose copyright is declared on the title page of this work, has granted to Simon Fraser University the right to lend this thesis, project or extended essay to users of the Simon Fraser University Library, and to make partial or single copies only for such users or in response to a request from the library of any other university, or other educational institution, on its own behalf or for one of its users.

The author has further granted permission to Simon Fraser University to keep or make a digital copy for use in its circulating collection (currently available to the public at the "Institutional Repository" link of the SFU Library website <www.lib.sfu.ca> at: <http://ir.lib.sfu.ca/handle/1892/112>) and, without changing the content, to translate the thesis/project or extended essays, if technically possible, to any medium or format for the purpose of preservation of the digital work.

The author has further agreed that permission for multiple copying of this work for scholarly purposes may be granted by either the author or the Dean of Graduate Studies.

It is understood that copying or publication of this work for financial gain shall not be allowed without the author's written permission.

Permission for public performance, or limited permission for private scholarly use, of any multimedia materials forming part of this work, may have been granted by the author. This information may be found on the separately catalogued multimedia material and in the signed Partial Copyright Licence.

The original Partial Copyright Licence attesting to these terms, and signed by this author, may be found in the original bound copy of this work, retained in the Simon Fraser University Archive.

Simon Fraser University Library
Burnaby, BC, Canada

Revised: Spring 2007

ABSTRACT

The osmium compounds $[Os_3(CO)_{10}PPh_2(CH_2)_4PPh_2]_2$ and $[Os_3(CO)_{10}PPh_2(CH_2)_6PPh_2]_2$ have been synthesized from $PPh_2(CH_2)_nPPh_2$ and $Os_3(CO)_{10}(MeCN)_2$. Spectroscopic evidence suggests the structure of each compound to be a dimer in which both phosphines of each of the bidentate $PPh_2(CH_2)_nPPh_2$ groups are bridged between adjacent osmium atoms on each of the osmium clusters.

The bidentate phosphine bridged compounds $Os_3(CO)_{11}PPh_2(CH_2)_nPPh_2M(CO)_5$ for M= Cr, Mo, and W (n = 1 - 6) have been synthesized from $Os_3(CO)_{11}PPh_2(CH_2)_nPPh_2$ and $M(CO)_5THF$. Structural data indicates that the uncoordinated phosphine of $Os_3(CO)_{11}PPh_2(CH_2)_nPPh_2$ acts as a typical donor ligand to the electron deficient metal centre of the $M(CO)_5$ unit.

The monosubstituted $[ReBr(CO)_4L]$ and bis-substituted $[ReBr(CO)_3L_2]$, where L is the ligand $Os_3(CO)_{11}PPh_2(CH_2)_nPPh_2$ (n = 2, 4), have been prepared from $Re(CO)_5Br$ and $Os_3(CO)_{11}PPh_2(CH_2)_nPPh_2$. The compound $Os_3(CO)_{11}PPh_2(CH_2)_nPPh_2Re(CO)_4Br$ is believed to have a *cis* conformation, while $[Os_3(CO)_{11}PPh_2(CH_2)_nPPh_2]_2Re(CO)_3Br$ is thought to have a *fac, cis* conformation.

DEDICATION

To my senior supervisor, Dr. R. K. Pomeroy, for giving me all the help and support that you were able to give, for your pitchers of beer on Friday afternoons, and for giving me the chance to prove that there was something between my ears after all.

To my committee members, especially Dr. R. Hill, who stepped up to the plate and assumed a much larger project than you had ever signed on for.

To my group members; thank you Richard for the wool sweater to blow my nose on and Craig for the occasional awkward pat on the back.

To my boyfriend Nathan for always believing in me and for bragging about me to your friends. To all the Tiessens for your love and family dinners.

Last but not least, to my parents for raising me to think for myself and to never be intimidated.

ACKNOWLEDGEMENTS

I wish to acknowledge the skilled technical assistance of Mr. Colin Zhang (NMR), Mr. Miki Yang (C/H/N), David McGillivray (LSIMS), Dr. Michael Jennings (X-ray Crystallography) and the secretarial staff in the Department of Chemistry at Simon Fraser University.

TABLE OF CONTENTS

LIST OF FIGURES

Figure **Page**

LIST OF TABLES

LIST OF SCHEMES

Scheme **Page**

LIST OF ABBREVIATIONS

LUMO	lowest unoccupied molecular orbital
HOMO	highest occupied molecular orbital
MeCN	acetonitrile, CH_3CN
Me_3NO	trimethylamine oxide, $(CH_3)_3NO$
THF	tetrahydrofuran
LSIMS	liquid secondary ion mass spectroscopy
NMR	nuclear magnetic resonance
mm	millimeters
fac	facial
mer	meridional

CHAPTER 1

INTRODUCTION

Metal Carbonyls[1]

The study of metal carbonyls is a specialized subsection of organometallic chemistry. Metal carbonyls have long been known to stabilize organic molecules, allowing for the isolation of compounds that would otherwise not be possible, to act as useful reagents in organic synthesis and to be catalytically active. Metal carbonyl clusters have the added advantage that ligands can be coordinated to one or more of the metal centres, allowing for a certain amount of control over their structure, spectroscopic properties and reactivity. A cluster is generally defined as a molecule containing three or more metal atoms connected by direct metal-metal bonds. Although clusters composed only of these skeletal metal atoms are known[1], most clusters are surrounded by a shell of ligands. Metal carbonyl clusters have many applications in chemistry, including their use as homogeneous catalysts, as precursors to metal nanoparticles on solid supports, as precursors to mononuclear or colloidal catalysts, and as structural models for chemisorption on metal surfaces.[1]

Group 6-9 transition metals form the most metal-carbonyl compounds because they have filled *d* orbitals of suitable energy to match the empty π^* LUMO on CO.

The first row transition metals on the left of the periodic table ($< d^6$) have few *d* electrons and therefore cannot tightly bind many carbonyl ligands.[2] The first row transition metals on the right of the periodic table (d^{10}) have *d* electrons too low in energy to interact effectively with the π^* LUMO on CO.[2] The first row transition metals in the centre of the periodic table (d^6-d^9) do have filled *d* orbitals of the correct energy to match the empty π* LUMO on CO, and thus many metals carbonyl compounds of groups 6-9 have been published.[2] There are many exceptions to these generalizations, as evidenced by compounds such as $[Ti(CO)_6]^{2-}$ and $[Hg(CO)_2]^{2+}$.

The second and third row transition metals follow a similar trend[2] since the separation between the *ns* and *np* atomic orbitals increases across the periodic table. This is because the *s* orbital is more penetrating than the *p* orbital and therefore an *s* electron experiences a greater effective nuclear charge as the atomic number increases (recall effective nuclear charge is equal to the atomic number minus the shielding constant).

Within group 8 it has been observed that $M_3(CO)_{12}$ where M= Ru or Os provide better models for the study of cluster chemistry than when M= Fe. For example, in the substitution of $Fe_3(CO)_{12,}$ reaction with a ligand at 50 °C produces a substituted metal cluster, but reaction at 80 °C causes the cluster to fragment. The Ru and Os analogues have less tendency to fragment, likely because their M-M bonds are stronger.[27] The reason for this is the cause of considerable disagreement among chemists, however it is often explained by two contributing factors: ground state destabilization and transition state stabilization. These two factors are represented pictorally in Figure 1.1 below.

Figure 1.1. Transition State Stabilization Verses Ground State Destabilization

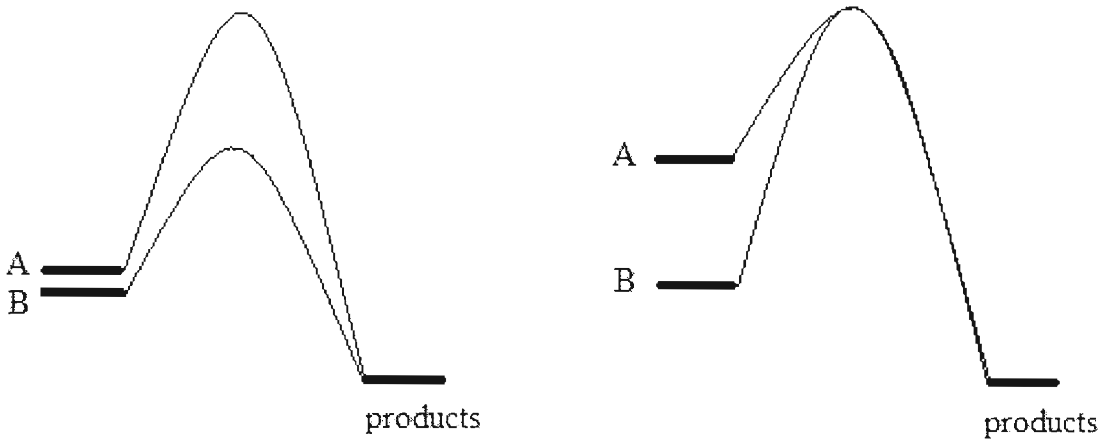

Transition State Stabilization

Ground State Destabilization

Transition State Stabilization

As shown in Figure 1.1, transition state destabilization occurs when reactants A and B have similar thermodynamic stability, but the transition state for reaction of A is at lower energy than that of reaction of B.

For example, the group 6 metal carbonyl compounds $Cr(CO)_6$, $Mo(CO)_6$, and $W(CO)_6$ all show a single carbonyl stretching mode at approximately 2000 cm^{-1} which indicates that the ground state M-CO bonds are of similar energy. The rate constants for substitution of this series with triphenylphosphine vary considerably;[3] at 130°C $Cr(CO)_6$ has $k_{sub}= 1.4 \times 10^{-4}$, $Mo(CO)_6$ has $k_{sub}= 2.0 \times 10^{-3}$ and $W(CO)_6$ has $k_{sub}= 4.0 \times 10^{-6}$. The lability of the metal carbonyl compounds in this example is due to transition state stabilization, but the exact reason for this trend is unknown.[3]

Ground State Destabilization

As shown in Figure 1.1, ground state destabilization occurs when reactant B is more thermodynamically stable than reactant A, thus decreasing the activation energy of reactant A and increasing its kinetic lability compared to that of reactant B.

For example, it is sometimes observed that the thermodynamic stability of M-M and M-C σ bonds of the third row transition metals are more stable than those of either the second or first rows, which is opposite to the main group trend. For example, in group 8 cluster stability of $M_3(CO)_{12}$ is in the order Os > Ru >> Fe.[4] While this often makes third row transition metal complexes unsuitable as catalysts, due to the high thermodynamic stability of the intermediates, it makes them ideal for the study of cluster chemistry since novel complexes can be isolated and characterized. The stability of third row transition metal complexes is often attributed to the combined effects of the lanthanide contraction and relativity.

The Lanthanide Contraction[5]

Third row transition metals have a complete *4f* shell; however, since shielding is in the order *s>p>d>f* the *f* orbitals do not screen the valence electrons very effectively and hence the valence orbitals are contracted. The effective nuclear charge Z_{eff} is much larger for the third row transition metals than for the first or second row due to the increased atomic number Z from the lanthanides and the low shielding S, since

$Z_{eff} = Z - S$. The end result of the lanthanide contraction is that the *6p, 6s*, and *5d* orbitals are lowered in energy so that there is better overlap of the third row transition metals with the bonding orbitals of carbon or other third row transition metals than there would be in the absence of the lanthanide contraction.

Figure 1.2 Effects of the Lanthanide Contraction on the Molecular Orbitals for a Metal-Ligand Interaction

Without the Lanthanide Contraction

With the Lanthanide Contraction

Relativity Effects[6]

It is known that when a nucleus has a high nuclear charge the speed of electrons close to the nucleus becomes comparable to the speed of light and consequently they gain mass. This effect becomes apparent in the third row transition metals and heavier elements. As a result of this effect the 6p and 6s orbitals contract and become lower in energy, while the 5d orbital is raised in energy due to the increased shielding by the contracted 6p and 6s electrons. This acts to raise the shielding constant S and lower Z_{eff}.

The lanthanide contraction and relativity effects combine to make the covalent radius of a third row transition metal in many cases almost identical to that of its second row analogue; in group 8 Fe has a metallic radius[7] of 1.26 Å, while that of Ru is 1.34 Å and that of Os is 1.35 Å. This rationale is often used to explain why third row transition metals form stronger M-CO and M-M bonds than would be expected.

The above reasons lead to the choice of $Os_3(CO)_{12}$ as the starting material in the following thesis, although it is expected that $Ru_3(CO)_{12}$ would exhibit similar chemistry.

$Os_3(CO)_{12}$

The simplest osmium carbonyl cluster is $Os_3(CO)_{12}$. This compound has a triangular metal skeleton with six equatorial and six axial carbonyls. The axial carbonyls are eclipsed, giving it D_{3h} symmetry.[8]

Figure 1.3. Structure of $Os_3(CO)_{12}$

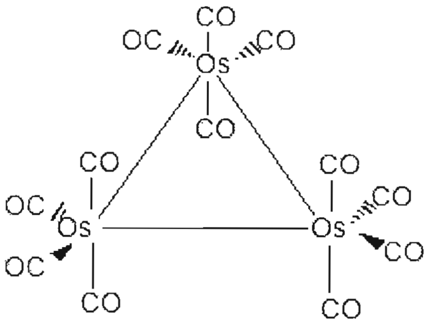

This compound is prepared by the reduction of osmium tetroxide in the presence of CO under pressure. This reaction is conducted in a bomb.

Scheme 1.1. Preparation of $Os_3(CO)_{12}$[9]

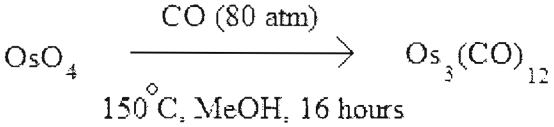

$$OsO_4 \xrightarrow[150^\circ C,\ MeOH,\ 16\ hours]{CO\ (80\ atm)} Os_3(CO)_{12}$$

π Backbonding in $Os_3(CO)_{12}$

The carbonyl ligand is primarily a π-accepter. The bonding interaction involves donation of electron density from the filled *3d* orbital on the osmium atom to the empty π* of the CO ligand.

Figure 1.4. σ-Donation and π-Backbonding in an Osmium-Carbonyl Interaction

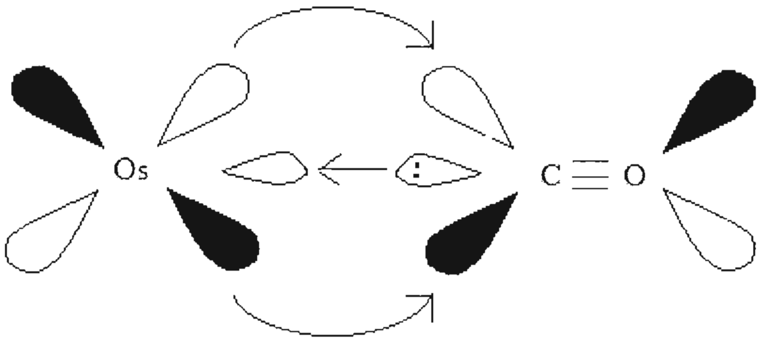

This population of the antibonding orbital on CO lowers the C-O bond order with respect to a free CO molecule, thus weakening and lengthening the CO bond. In terms of spectroscopy, this bonding effect can be observed in the lowering of the IR frequency of the CO stretching modes in $Os_3(CO)_{12}$ from those of free CO.

Phosphine Ligands

The addition of phosphine ligands to the osmium cluster $Os_3(CO)_{12}$ has been of interest to cluster chemists since the development of the activated clusters $Os_3(CO)_{11}(MeCN)$ and $Os_3(CO)_{10}(MeCN)_2$ by Johnson, Lewis and Pippard in 1981.[10] The $Os_3(CO)_{12}$ cluster is treated with one or two equivalents of Me_3NO and MeCN to prepare the activated clusters of $Os_3(CO)_{11}(MeCN)$ and $Os_3(CO)_{10}(MeCN)_2$, respectively. The monosubstituted cluster has the advantage of having only one labile site and hence reaction with a phosphine yields only the monosubstituted product.

Scheme 1.2. Reaction of $Os_3(CO)_{11}(MeCN)$ with a Phosphine

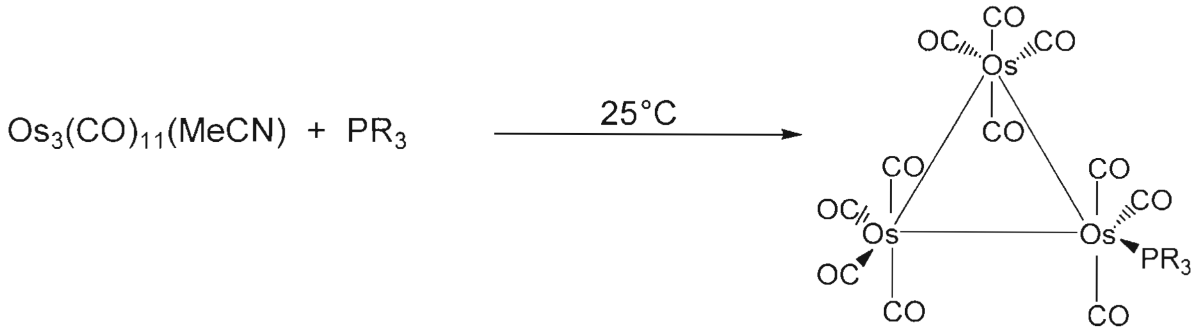

Similarly, reaction of the bis-substituted cluster with two equivalents of phosphine yields only the bis-substituted product.

Scheme 1.3. Reaction of $Os_3(CO)_{10}(MeCN)_2$ with a Phosphine

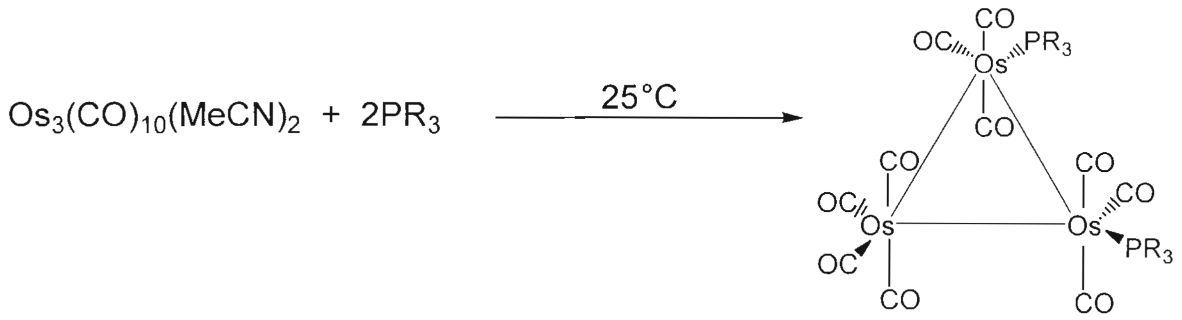

Since the first report of this reaction a plethora of clusters of the type $Os_3(CO)_{11}(L)$ and $Os_3(CO)_{10}(L)_2$ have been synthesized.

History of the $PPh_2(CH_2)_nPPh_2$ Ligand in Relation to Osmium Clusters

Of particular interest are phosphine ligands which have the capacity to be monodentate or bidentate, such as $PPh_2(CH_2)_nPPh_2$. In 1984, Clucas *et al.*.[11] reported the synthesis of $Os_3(CO)_{10}(\mu\text{-}PPh_2CH_2PPh_2)$ in which the phosphine ligand bridges two osmium atoms and each phosphine occupies an equatorial site on the cluster. Clucas *et al.* also reported its pyrolysis product, $Os_3(CO)_8(H)(Ph_2PCH_2P(Ph)C_6H_4)$ in which two CO ligands have been lost and one of the phenyl groups has become metallated. Also in

1984, Poe and Sekhar[12] reported the preparation of $Os_3(CO)_{11}(\eta^1\text{-}PPh_2CH_2PPh_2)$ in which one of the phosphorus atoms is coordinated to an osmium atom in an equatorial position and the other phosphorus atom is dangling free. They also studied its kinetic conversion to $Os_3(CO)_{10}(\mu\text{-}PPh_2CH_2PPh_2)$. Further in 1984, Deeming *et al.*[13] reported the synthesis of $Os_3(CO)_{10}(\mu\text{-}PPh_2(CH_2)_nPPh_2)$ with $n = 1 - 4$ and identified both bridging and chelating isomers. They found that the shorter the carbon chain on the $PPh_2(CH_2)_nPPh_2$ ligand, the greater the tendency to form the bridging isomer. The chelating isomer, that is, the isomer in which both phosphorus atoms are coordinated to the same osmium atom, becomes more prevalent as the carbon chain increases in length. In 1985, Cartwright *et al.*[14] reported the synthesis of $Os_3(CO)_8(\mu\text{-}PPh_2CH_2PPh_2)_2$ and the synthesis and crystal structure of $Os_3(CO)_9(\mu\text{-}PPh_2CH_2PPh_2)(\eta^1\text{-}PPh_2CH_2PPh_2)$. In 1987, Deeming *et al.*[15] reported two more new types of compounds: $Os_3(CO)_{11}PPh_2(CH_2)_nPPh_2$ ($n = 1 - 4$) and $Os_3(CO)_{11}PPh_2(CH_2)_nPPh_2Os_3(CO)_{11}$ ($n = 2 - 4$), in which the bidentate phosphine acts as a bridge between the two osmium clusters. The compound $Os_3(CO)_{11}PPh_2(CH_2)_nPPh_2Os_3(CO)_{11}$ ($n = 1$) was not synthesized despite attempts,[15] probably because $Os_3(CO)_{11}PPh_2CH_2PPh_2$ undergoes decarbonylation to form $Os_3(CO)_{10}(\mu\text{-}PPh_2CH_2PPh_2)$ at a much faster rate than to displace another molecule of MeCN from $Os_3(CO)_{11}(MeCN)$ to form $Os_3(CO)_{11}PPh_2CH_2PPh_2Os_3(CO)_{11}$. Also in 1987, Deeming *et al.*[16] reported the protonation and hydrogenation products of $Os_3(CO)_{10}(\mu\text{-}PPh_2CH_2PPh_2)$ ($n = 1 - 4$) which are $[Os_3(\mu\text{-}H)(CO)_{10}(PPh_2(CH_2)_nPPh_2)]^+$ and $[Os_3(\mu\text{-}H)_2(CO)_8(PPh_2(CH_2)_nPPh_2)]$, respectively. In 1988 Deeming *et al.*[17] presented a crystal structure of $Os_3(CO)_{10}(\mu\text{-}PPh_2(CH_2)_nPPh_2)$ for $n = 2$, and later in 1995[18] they presented the corresponding structures for the $n = 4$ and $n = 5$ analogues.

Thesis Goals

Although clusters of the type $Os_3(CO)_{10}(\mu\text{-}PPh_2(CH_2)_nPPh_2)$ have been quite thoroughly studied, there has been far less attention given to clusters of the type $Os_3(CO)_{11}PPh_2(CH_2)_nPPh_2$ and $Os_3(CO)_{11}PPh_2(CH_2)_nPPh_2Os_3(CO)_{11}$. The goals of this thesis are manifold.

The first goal is to repeat the preparation of the compound $Os_3(CO)_{11}PPh_2(CH_2)_nPPh_2$ (n = 1 - 5) published by Deeming *et al.* in the hopes of improving the synthesis and completing the characterization with X-ray crystallography. I also wish to prepare and characterize $Os_3(CO)_{11}PPh_2(CH_2)_6PPh_2$ in which the carbon chain is further extended.

The second goal is to repeat the preparation of the compound $Os_3(CO)_{11}PPh_2(CH_2)_nPPh_2Os_3(CO)_{11}$ (n = 2 - 5) published by Deeming *et al.*, also with the objective of improving the synthesis and completing the characterization with X-ray crystallography. I further wish to attempt to prepare $Os_3(CO)_{11}PPh_2CH_2PPh_2Os_3(CO)_{11}$ which Deeming *et al.* failed to synthesize, and to prepare and characterize $Os_3(CO)_{11}PPh_2(CH_2)_6PPh_2Os_3(CO)_{11}$.

The third goal is to explore the possibility of preparing a double bridged system of the type $Os_3(CO)_{10}[PPh_2(CH_2)_nPPh_2]_2Os_3(CO)_{10}$ and to vary the carbon chain length by using a medium and long carbon chain.

The fourth goal is to coordinate various transition metal accepting groups to the dangling phosphine of $Os_3(CO)_{11}PPh_2(CH_2)_nPPh_2$ including $Cr(CO)_5$, $Mo(CO)_5$, $W(CO)_5$, and $Re(CO)_4Br$, while simultaneously varying the carbon chain length from one to six carbons in the bidentate phosphine.

The fifth goal is to coordinate two and three units of $Os_3(CO)_{11}PPh_2(CH_2)_nPPh_2$ to the transition metal centres $Re(CO)_3Br$ and $Re(CO)_2Br$, respectively.

Herein is presented $Os_3(CO)_{11}PPh_2(CH_2)_nPPh_2$ ($n = 1 - 6$) and its osmium, rhenium, and group 6 derivatives.

CHAPTER 2

$Os_3(CO)_{11}PPh_2(CH_2)_nPPh_2$ AND THE OSMIUM DERIVATIVES $Os_3(CO)_{11}PPh_2(CH_2)_nPPh_2Os_3(CO)_{11}$ AND $[Os_3(CO)_{10}PPh_2(CH_2)_nPPh_2]_2$

2.1. Introduction

The first target of this chapter is to repeat the preparation of the compound $Os_3(CO)_{11}PPh_2(CH_2)_nPPh_2$ (n = 1 - 5) published by Deeming *et al.* with the goal of improving the synthesis and completing the characterization to include an X-ray crystal structure of $Os_3(CO)_{11}PPh_2(CH_2)_2PPh_2$. Also presented is the preparation and characterization of $Os_3(CO)_{11}PPh_2(CH_2)_6PPh_2$ in which the carbon chain is further extended. These six compounds are used as starting materials for compounds presented later in chapters three and four.

The second target of this chapter is to repeat the preparation of the compound $Os_3(CO)_{11}PPh_2(CH_2)_nPPh_2Os_3(CO)_{11}$ (n = 2 - 5) published by Deeming *et al.*, also with the objective of improving the synthesis and completing the characterization to include X-ray crystal structures of $Os_3(CO)_{11}PPh_2(CH_2)_2PPh_2Os_3(CO)_{11}$ and $Os_3(CO)_{11}PPh_2(CH_2)_4PPh_2Os_3(CO)_{11}$. Furthermore, an attempt to prepare $Os_3(CO)_{11}PPh_2CH_2PPh_2Os_3(CO)_{11}$ which Deeming *et al.* failed to synthesize is discussed, and the preparation and characterization $Os_3(CO)_{11}PPh_2(CH_2)_6PPh_2Os_3(CO)_{11}$ is shown.

The third target of this chapter is to prepare a double bridged system of the type $Os_3(CO)_{10}[\mu\text{-}PPh_2(CH_2)_nPPh_2]_2Os_3(CO)_{10}$ and to vary the carbon chain length by using a medium (n = 4) and long (n = 6) carbon chain. The proposed structure for these compounds contains unusual rings of osmium, phosphorus and carbon atoms, with ring sizes of 16 and 20 atoms, respectively.

2.2. Results

2.2.1. $Os_3(CO)_{11}PPh_2(CH_2)_nPPh_2$

2.2.1.1. Synthesis of $Os_3(CO)_{11}PPh_2(CH_2)_nPPh_2$

The compound $Os_3(CO)_{11}PPh_2(CH_2)_4PPh_2$ was prepared by adding in small aliquots of $Os_3(CO)_{11}(MeCN)$ dissolved in dichloromethane to a stirring solution of $PPh_2(CH_2)_4PPh_2$ in dichloromethane. The solvent was removed and the solid was purified by column chromatography then recrystallized by slow cooling in hexanes to produce orange crystals.

The compounds $Os_3(CO)_{11}PPh_2(CH_2)_nPPh_2$ (n = 1 - 3 and 5 - 6) were prepared in a similar manner. They ranged from orange to red solids with increasing n values. They appeared to be stable under nitrogen at room temperature for several weeks.

The compounds were analyzed by infrared spectroscopy in hexanes solution. The absorptions in the carbonyl region for $Os_3(CO)_{11}PPh_2(CH_2)_4PPh_2$ are as follows: 2108 (w), 2055 (m), 2035 (m), 2020 (s), 2002 (w), 1991 (m), 1981 (w,b) cm^{-1}.

The IR stretches due to the carbonyls on the osmium cluster in $Os_3(CO)_{11}PPh_2(CH_2)_nPPh_2$ agree with those published by Deeming *et al.*[15] and are typical for a monophosphine substituted triosmium cluster. The stretching frequencies match closely to those of $Os_3(CO)_{11}PPh_3$ for example [2108(m), 2055(m), 2035(ms), 2019(s), 2000(m), 1989(m), 1978(m), 1956(w) cm^{-1}].[19] Although the weak band at 1956 cm^{-1} is not visible in the spectrum of $Os_3(CO)_{11}PPh_2(CH_2)_4PPh_2$, it is most likely present but hidden by the broad band at 1981 cm^{-1}; indeed the visual picture of these two spectra is very similar (see Appendix) and the apparent difference in their number of bands is more likely attributed to the quality of the infrared spectra rather than any difference in their compound structures.

The compounds $Os_3(CO)_{11}PPh_2(CH_2)_nPPh_2$ (n = 1 – 3 and 5 - 6) show similar absorptions. The carbonyl absorptions do not vary with the length of the carbon chain of the bidentate phosphine.

The compounds $Os_3(CO)_{11}PPh_2(CH_2)_nPPh_2$ (n = 1 - 6) were analyzed by mass spectroscopy. Their molecular weights are tabulated in Table 2.1 below.

Table 2.1. Mass Spectroscopic Data for $Os_3(CO)_{11}PPh_2(CH_2)_nPPh_2$

Compound	**n Value**	**Molecular Weight**	
		Calculated	**Observed**
$Os_3(CO)_{11}PPh_2(CH_2)_nPPh_2$	1	1264	1263.8
	2	1278	1275.8
	4	1306	1304.7
	5	1320	1319.7

The mass spectra of $Os_3(CO)_{11}PPh_2(CH_2)_3PPh_2$ and $Os_3(CO)_{11}PPh_2(CH_2)_6PPh_2$ did not show a molecular ion peak. The reason for this is not known.

In some cases there are slight variations between the calculated molecular weight and the observed molecular weight, particularly in compounds $Os_3(CO)_{11}PPh_2(CH_2)_2PPh_2$ and $Os_3(CO)_{11}PPh_2(CH_2)_4PPh_2$. This apparent inconsistency can be attributed to variability in the technique used to generate the spectra and is not unusual.[20]

The compound $Os_3(CO)_{11}PPh_2(CH_2)_2PPh_2$ was analyzed by elemental analysis. The observed % carbon was 34.66 and % hydrogen was 1.81, in agreement with the calculated values of 34.79 % carbon and 1.89 % hydrogen for the empirical formula $Os_3P_2C_{37}O_{11}H_{24}$.

2.2.1.2. Structural Determination of $Os_3(CO)_{11}PPh_2(CH_2)_2PPh_2$

The structure of compound $Os_3(CO)_{11}PPh_2(CH_2)_2PPh_2$ was determined by X-ray crystallography. A view of the molecule is shown in Figure 2.1. Some bond length and angle data are given in Table 2.2.

As can be seen from the figure, one phosphine is bonded to an osmium atom in an equatorial position, as would be expected for a bulky ligand, while the second phosphine is not coordinated. This is consistent with the structure proposed by Deeming *et al.*.[15]

The Os-P bond length is 2.349(2) Å, whereas in $Os_3(CO)_{11}PPh_3$ the Os-P bond length is 2.370(2). This decrease in bond length is consistent with $PPh_2(CH_2)_nPPh_2$ having a smaller cone angle[21] than PPh_3.

In the parent carbonyl $Os_3(CO)_{12}$ the Os-Os bond lengths average 2.877Å with one bond being longer than the other two. In monophosphine substituted compounds such as $Os_3(CO)_{11}L$ where L = PPh_3, $P(OMe)_3$, $PPh(OMe)_2$, it is observed that the Os-Os bond *cis* to the phosphine is the longest of the three.[21] The same trend was observed in compound $Os_3(CO)_{11}PPh_2(CH_2)_2PPh_2$, where the metal-metal bond *cis* to the phosphine was 2.9025(5) Å, while the other two metal-metal bonds were 2.8888(5) Å and 2.8721(5) Å. Bruce *et al.*[21] have suggested that this is due to steric interactions between the phosphine and the CO group *cis* to it on the adjacent Os atom. As further evidence for this rationale, they noted that the lengthening increases with increased cone angle of the phosphine.

It is observed in the parent carbonyl $Os_3(CO)_{12}$ as well as in various monophosphine-substituted triosmium compounds that the bonds from the metal atoms to the axial carbonyls are longer than those to the equatorial carbonyls.[21] This trend is also observed in compound $Os_3(CO)_{11}PPh_2(CH_2)_2PPh_2$, in which the average M-CO_{ax} distances are 1.931 Å while the average M-CO_{eq} distances are 1.916 Å. This phenomenon has been interpreted previously[14] as reflecting the differences in degrees of backbonding between two mutually *trans* CO ligands (axial) verses a CO *trans* to a metal-metal bond (equatorial). The *trans* axial CO ligands have a greater competition for backbonding electron density than the equatorial ligands and their *trans* metal atoms.

The axial carbonyls of the osmium cluster have a staggered conformation, with the axial carbonyls on Os2 and Os3 leaning inward towards the phosphine substituted Os1 atom. This is different than in the basic $Os_3(CO)_{12}$ cluster where the axial carbonyls are almost perfectly eclipsed. This phenomenon is not unusual among phosphine substituted triosmium clusters and is thought to relieve the steric strain introduced by coordination of the phosphine ligand.[21]

The *trans* axial carbonyls are also slightly bent, with bond angles of 173-178°, with the axial carbonyls of Os3, which is on the same side of the cluster as the phosphine, being the most bent (173°). This has also been observed in other monophosphine-substituted triosmium clusters.[21]

Figure 2.1. Crystal Structure of $Os_3(CO)_{11}PPh_2(CH_2)_2PPh_2$

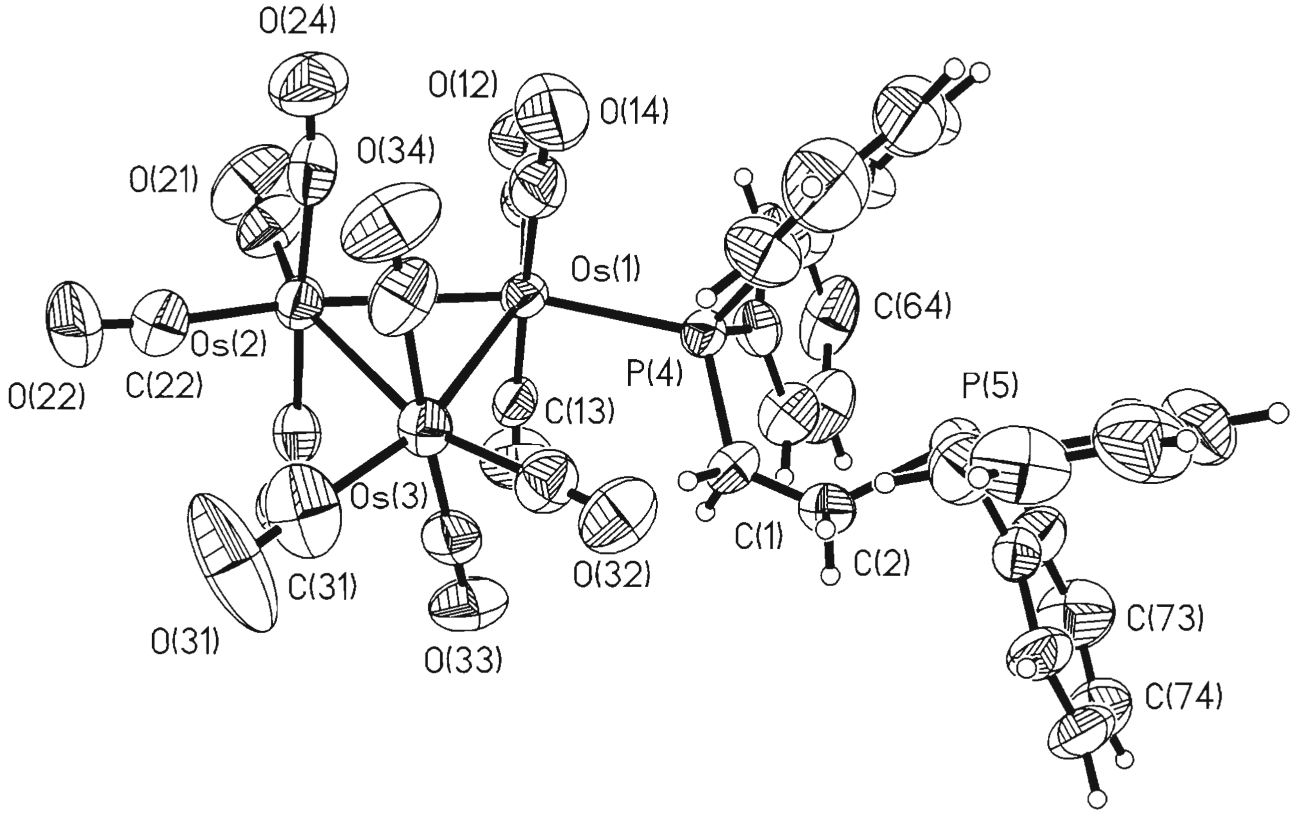

Table 2.2. Selected Bond Lengths and Angles for $Os_3(CO)_{11}PPh_2(CH_2)_2PPh_2$

Bond Lengths (Å)

Os(1) – C(12)	1.889(10)	P(4) – C(1)	1.816(8)
Os(1) – C(14)	1.901(10)	C(1) – C(2)	1.326(10)
Os(1) – C(13)	1.920(9)	P(5) – C(2)	1.843(9)
Os(1) – P(4)	2.349(2)	C(12) – O(12)	1.150(10)
Os(1) – Os(2)	2.8721(5)	C(13) – O(13)	1.150(9)
Os(1) – Os(3)	2.9025(5)	C(14) – O(14)	1.153(10)
Os(2) – C(24)	1.920(11)	C(21) – O(21)	1.122(11)
Os(2) – C(22)	1.928(12)	C(22) – O(22)	1.124(11)
Os(2) – C(21)	1.938(11)	C(23) – O(23)	1.135(10)
Os(2) – C(23)	1.952(11)	C(24) – O(24)	1.149(11)
Os(2) – Os(3)	2.8888(5)	C(31) – O(31)	1.116(13)
Os(3) – C(32)	1.903(10)	C(32) – O(32)	1.127(10)
Os(3) – C(31)	1.922(13)	C(33) – O(33)	1.139(9)
Os(3) – C(33)	1.942(10)	C(34) – O(34)	1.132(11)
Os(3) – C(34)	1.952(11)		

Bond Angles (deg)

C(12)-Os(1)-C(14)	91.4(4)	C(23)-Os(2)-Os(1)	92.3(3)
C(12)-Os(1)-C(13)	89.9(4)	C(24)-Os(2)-Os(3)	93.1(3)
C(14)-Os(1)-C(13)	178.1(4)	C(22)-Os(2)-Os(3)	97.9(3)
C(12)-Os(1)-P(4)	99.8(3)	C(21)-Os(2)-Os(3)	159.2(3)
C(14)-Os(1)-P(4)	90.8(3)	C(23)-Os(2)-Os(3)	84.1(3)
C(13)-Os(1)-P(4)	87.6(2)	Os(1)-Os(2)-Os(3)	60.507(12)
C(12)-Os(1)-Os(2)	95.8(3)	C(32)-Os(3)-C(31)	99.8(4)
C(14)-Os(1)-Os(2)	92.8(3)	C(32)-Os(3)-C(33)	91.1(4)
C(13)-Os(1)-Os(2)	88.4(2)	C(31)-Os(3)-C(33)	92.7(4)
P(4)-Os(1)-Os(2)	163.86(5)	C(32)-Os(3)-C(34)	91.2(4)
C(12)-Os(1)-Os(3)	155.4(3)	C(31)-Os(3)-C(34)	93.1(5)
C(14)-Os(1)-Os(3)	85.7(3)	C(33)-Os(3)-C(34)	173.3(4)
C(13)-Os(1)-Os(3)	93.7(2)	C(32)-Os(3)-Os(2)	162.6(3)
P(4)-Os(1)-Os(3)	104.66(5)	C(31)-Os(3)-Os(2)	97.1(3)
Os(2)-Os(1)-Os(3)	60.032(12)	C(33)-Os(3)-Os(2)	92.6(2)
C(24)-Os(2)-C(22)	89.1(4)	C(34)-Os(3)-Os(2)	83.4(3)
C(24)-Os(2)-C(21)	90.0(4)	C(32)-Os(3)-Os(1)	104.3(3)
C(22)-Os(2)-C(21)	102.7(5)	C(31)-Os(3)-Os(1)	155.5(3)
C(24)-Os(2)-C(23)	176.1(4)	C(33)-Os(3)-Os(1)	82.1(2)
C(22)-Os(2)-C(23)	93.9(4)	C(34)-Os(3)-Os(1)	91.2(3)
C(21)-Os(2)-C(23)	91.6(4)	Os(2)-Os(3)-Os(1)	59.461(12)
C(24)-Os(2)-Os(1)	83.9(3)	C(1)-P(4)-Os(1)	112.8(3)
C(22)-Os(2)-Os(1)	156.7(3)	C(2)-C(1)-P(4)	127.5(7)
C(21)-Os(2)-Os(1)	99.4(3)	C(1)-C(2)-P(5)	126.5(7)

2.2.2. $Os_3(CO)_{11}PPh_2(CH_2)_nPPh_2Os_3(CO)_{11}$

2.2.2.1. Synthesis of $Os_3(CO)_{11}PPh_2(CH_2)_nPPh_2Os_3(CO)_{11}$

The compound $Os_3(CO)_{11}PPh_2(CH_2)_4PPh_2Os_3(CO)_{11}$ was prepared by adding $PPh_2(CH_2)_4PPh_2$ to $Os_3(CO)_{11}(MeCN)$ in dichloromethane at room temperature. The solvent was removed and the solid was purified by column chromatography then recrystallized from CH_2Cl_2 / hexanes to produce yellow crystals.

The compounds $Os_3(CO)_{11}PPh_2(CH_2)_nPPh_2Os_3(CO)_{11}$ (n = 2 - 3 and 5 - 6) were prepared in a similar manner. In each case the result was yellow crystals, except for compound $Os_3(CO)_{11}PPh_2(CH_2)_3PPh_2Os_3(CO)_{11}$, which could not be crystallized. Attempts to prepare $Os_3(CO)_{11}PPh_2CH_2PPh_2Os_3(CO)_{11}$ were unsuccessful.

The compounds were analyzed by infrared spectroscopy in hexanes solution and the carbonyl absorptions for $Os_3(CO)_{11}PPh_2(CH_2)_4PPh_2Os_3(CO)_{11}$ are as follows: 2108 (w), 2055 (m), 2035 (m), 2020 (s), 2002 (w), 1991 (m), 1982 (w,b) cm^{-1}.

The IR stretches due to the carbonyls on the osmium cluster in $Os_3(CO)_{11}PPh_2(CH_2)_4PPh_2Os_3(CO)_{11}$ agree with those published by Deeming *et al.*[9] and are typical for a monophosphine substituted triosmium cluster.

As expected the absorptions do not vary from those of $Os_3(CO)_{11}PPh_2(CH_2)_4PPh_2$. For example, the band at 2020 cm^{-1} in the spectrum of $Os_3(CO)_{11}PPh_2(CH_2)_4PPh_2Os_3(CO)_{11}$ is also found at 2020 cm^{-1} in the spectrum of $Os_3(CO)_{11}PPh_2(CH_2)_4PPh_2$.

The compounds $Os_3(CO)_{11}PPh_2(CH_2)_nPPh_2Os_3(CO)_{11}$ (n = 2 - 3, 5 - 6) show similar absorptions, which do not vary with the length of the carbon chain. For example, the band at 2020 cm^{-1} in the spectrum of $Os_3(CO)_{11}PPh_2(CH_2)_4PPh_2Os_3(CO)_{11}$ ranges from 2019 to 2020 cm^{-1} for the compounds $Os_3(CO)_{11}PPh_2(CH_2)_nPPh_2Os_3(CO)_{11}$ (n = 2 - 3, 5 - 6), well within the error limit of 2 cm^{-1} for the instrument.

The compounds $Os_3(CO)_{11}PPh_2(CH_2)_nPPh_2Os_3(CO)_{11}$ (n = 2 - 6) were analyzed by $^{31}P\{^1H\}$ NMR Spectroscopy. Their chemical shifts are tabulated in Table 2.3 below.

Table 2.3. $^{31}P\{^1H\}$ NMR Data of $Os_3(CO)_{11}PPh_2(CH_2)_nPPh_2Os_3(CO)_{11}$

Compound	n Value	^{31}P NMR Resonances
$Os_3(CO)_{11}PPh_2(CH_2)_nPPh_2Os_3(CO)_{11}$	2	-8.7 (s)
	3	-8.6 (s)
	4	-8.3 (s)
	5	-7.3 (s)
	6	-8.2 (s)

The compounds $Os_3(CO)_{11}PPh_2(CH_2)_nPPh_2Os_3(CO)_{11}$ (n = 2 - 6) show a single resonance indicating that both phosphorus atoms in the molecule are equivalent. The chemical shift values do not vary significantly with the carbon chain length and are consistent with those reported by Deeming *et al.*.[15]

The compounds $Os_3(CO)_{11}PPh_2(CH_2)_nPPh_2Os_3(CO)_{11}$ (n = 2 - 6) were analyzed by mass spectroscopy. Their observed molecular weights are tabulated in Table 2.4 below.

Table 2.4. Mass Spectroscopic Data of $Os_3(CO)_{11}PPh_2(CH_2)_nPPh_2Os_3(CO)_{11}$

Compound	n Value	Molecular Weight	
		Calculated	Observed
$Os_3(CO)_{11}PPh_2(CH_2)_nPPh_2Os_3(CO)_{11}$	2	2156	2155.1
	3	2170	2171.7
	4	2184	2184.4
	5	2198	2197.6
	6	2212	2213.5

Although there are some slight variations due to variability in the technique used to generate the spectra,[20] the observed molecular weights agree with the calculated molecular weights for the compounds $Os_3(CO)_{11}PPh_2(CH_2)_nPPh_2Os_3(CO)_{11}$ (n = 2 - 6).

The compounds $Os_3(CO)_{11}PPh_2(CH_2)_nPPh_2Os_3(CO)_{11}$ (n=2,4-6) were analyzed by elemental analysis. $Os_3(CO)_{11}PPh_2(CH_2)_3PPh_2Os_3(CO)_{11}$ was not analyzed because it could not be obtained with suitable purity. The results of elemental analysis are tabulated below in Table 2.5.

Table 2.5. Elemental Analysis Data of $Os_3(CO)_{11}PPh_2(CH_2)_nPPh_2Os_3(CO)_{11}$

Compound	n Value	Elemental Analysis			
		Calculated		Observed	
		% C	% H	% C	% H
$Os_3(CO)_{11}PPh_2(CH_2)_nPPh_2Os_3(CO)_{11}$	2	26.74	1.12	26.63	1.24
	4	27.50	1.29	27.86	1.38
	5	27.87	1.38	27.79	1.46
	6	28.23	1.46	28.46	1.60

The observed % carbon and % hydrogen agree within uncertainty to the calculated values for the empirical formula of the compounds $Os_3(CO)_{11}PPh_2(CH_2)_nPPh_2Os_3(CO)_{11}$ (n = 2, 4 - 6).

2.2.2.2. Structural Determination of $Os_3(CO)_{11}PPh_2(CH_2)_2PPh_2Os_3(CO)_{11}$ and $Os_3(CO)_{11}PPh_2(CH_2)_4PPh_2Os_3(CO)_{11}$

The structure of compounds $Os_3(CO)_{11}PPh_2(CH_2)_2PPh_2Os_3(CO)_{11}$ and $Os_3(CO)_{11}PPh_2(CH_2)_4PPh_2Os_3(CO)_{11}$ was determined by X-ray crystallography. Views of the molecules are shown in Figure 2.2 (n = 2) and Figure 2.3 (n = 4). Some bond length and angle data are given in Table 2.6 (n = 2) and Table 2.7 (n = 4).

The crystal used in structural analysis of $Os_3(CO)_{11}PPh_2(CH_2)_2PPh_2Os_3(CO)_{11}$ was of poor quality and diffracted weakly. Furthermore, there was not enough data obtained during analysis. For these reasons, X-ray crystallography of $Os_3(CO)_{11}PPh_2(CH_2)_2PPh_2Os_3(CO)_{11}$ produced a crystal structure with a high R factor of 0.1120 (see Appendix). Although selected bond lengths and angles are reported in Table 2.6, the only reliable information derived from this structural analysis is the connectivity of the atoms.

The R factor for the X-ray crystal structure of $Os_3(CO)_{11}PPh_2(CH_2)_4PPh_2Os_3(CO)_{11}$ was much lower, at a value of 0.0696. Consequently the selected bond lengths and angles listed in Table 2.7 are meaningful.

The crystal structure of compound $Os_3(CO)_{11}PPh_2(CH_2)_2PPh_2Os_3(CO)_{11}$ shows a monophosphine substituted triosmium cluster with the dangling phosphine coordinated to a second triosmium cluster, as suggested by Deeming *et al.*[15]

The crystal structure of $Os_3(CO)_{11}PPh_2(CH_2)_4PPh_2Os_3(CO)_{11}$ shows a structure analogous to that of $Os_3(CO)_{11}PPh_2(CH_2)_2PPh_2Os_3(CO)_{11}$.

In $Os_3(CO)_{11}PPh_2(CH_2)_4PPh_2Os_3(CO)_{11}$ the axial carbonyls on Os2, being on the same side of the cluster as the phosphorus atom P1, are the most bent at a *trans* axial bond angle of 172°. The phosphine P1 is pushed down out of the plane of the triosmium cluster while the equatorial carbonyl C13 is raised slightly above the plane, with respect to the view of the molecule shown in Figure 2.3. The compound $Os_3(CO)_{11}PPh_2(CH_2)_4PPh_2Os_3(CO)_{11}$ also shows a staggering of its axial carbonyls. The carbonyl C21 is leaning inwards towards Os1 and Os3 while its *trans* axial carbonyl C22 is leaning towards the phosphine substituted Os1 but away from Os3. The axial carbonyl

Figure 2.2. Crystal Structure of $Os_3(CO)_{11}PPh_2(CH_2)_2PPh_2Os_3(CO)_{11}$

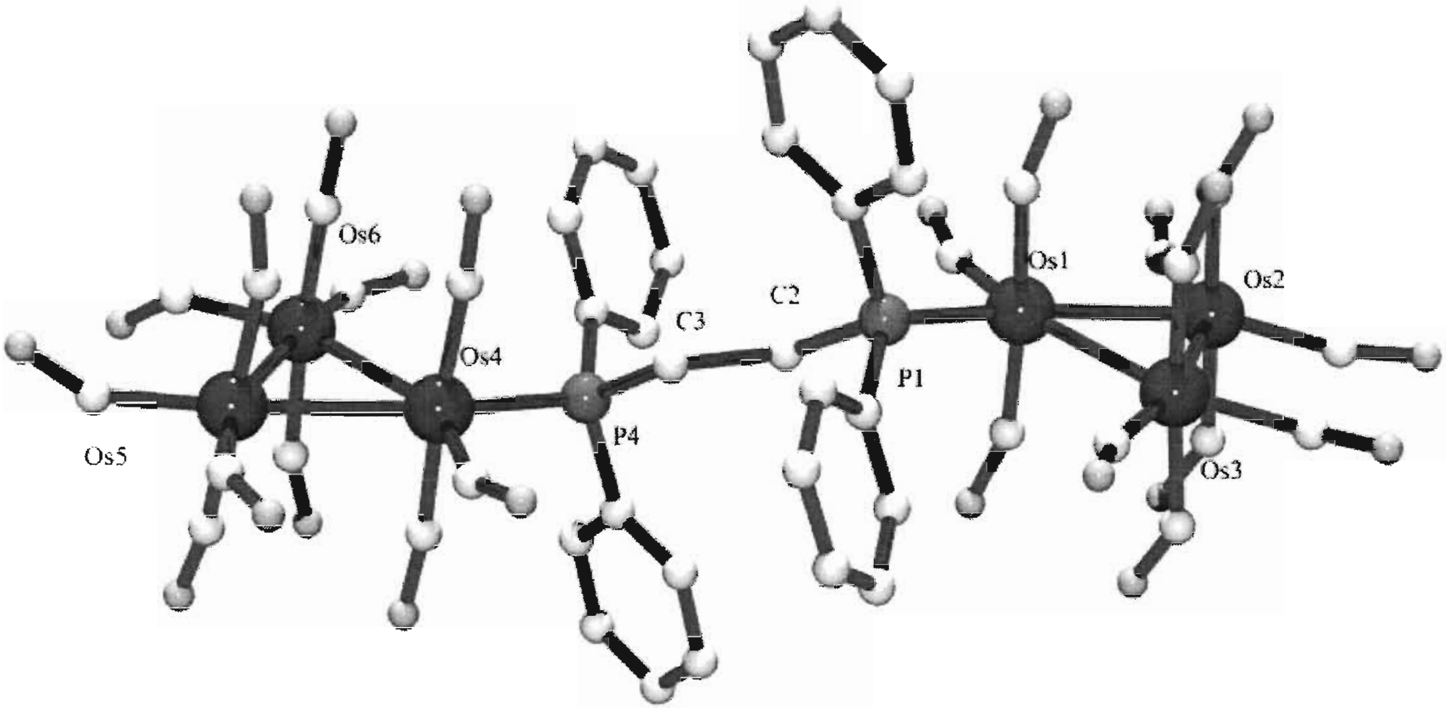

Table 2.6. Selected Bond Lengths and Angles for $Os_3(CO)_{11}PPh_2(CH_2)_2PPh_2Os_3(CO)_{11}$

Bond Lengths (Å)

Os(1)-C(13)	1.87(2)	Os(6)-C(63)	1.89(2)
Os(1)-C(12)	1.88(2)	Os(6)-C(61)	1.89(2)
Os(1)-C(11)	1.88(2)	P(1)-C(2)	1.71(7)
Os(1)-P(1)	2.284(17)	C(2)-C(3)	1.70(7)
Os(1)-Os(2)	2.872(4)	C(3)-P(4)	1.73(8)
Os(1)-Os(3)	2.879(5)	C(11)-O(11)	1.20(2)
Os(2)-C(24)	1.90(3)	C(12)-O(12)	1.198(19)
Os(2)-C(23)	1.92(3)	C(13)-O(13)	1.20(2)
Os(2)-C(21)	1.92(3)	C(21)-O(21)	1.21(2)
Os(2)-C(22)	1.93(3)	C(22)-O(22)	1.21(2)
Os(2)-Os(3)	2.867(4)	C(23)-O(23)	1.21(2)
Os(3)-C(32)	1.94(2)	C(24)-O(24)	1.20(2)
Os(3)-C(34)	1.95(2)	C(31)-O(31)	1.200(19)
Os(3)-C(33)	1.95(3)	C(32)-O(32)	1.19(2)
Os(3)-C(31)	1.96(2)	C(33)-O(33)	1.21(2)
Os(4)-C(43)	1.88(2)	C(34)-O(34)	1.21(2)
Os(4)-C(42)	1.88(2)	C(41)-O(41)	1.20(2)
Os(4)-C(41)	1.88(2)	C(42)-O(42)	1.21(2)
Os(4)-P(4)	2.36(2)	C(43)-O(43)	1.20(2)
Os(4)-Os(5)	2.873(5)	C(51)-O(51)	1.21(2)
Os(4)-Os(6)	2.893(6)	C(52)-O(52)	1.206(19)
Os(5)-C(51)	1.90(2)	C(53)-O(53)	1.21(2)
Os(5)-C(54)	1.90(3)	C(54)-O(54)	1.21(2)
Os(5)-C(53)	1.90(2)	C(61)-O(61)	1.22(2)
Os(5)-C(52)	1.91(2)	C(62)-O(62)	1.227(19)
Os(5)-Os(6)	2.882(5)	C(63)-O(63)	1.21(2)
Os(6)-C(62)	1.88(2)	C(64)-O(64)	1.21(2)
Os(6)-C(64)	1.88(2)		

Bond Angles (deg)

C(13)-Os(1)-C(12)	91(3)	C(42)-Os(4)-C(41)	176(2)
C(13)-Os(1)-C(11)	90(4)	C(43)-Os(4)-P(4)	103(2)
C(12)-Os(1)-C(11)	175(3)	C(42)-Os(4)-P(4)	88.6(15)
C(13)-Os(1)-P(1)	93.1(17)	C(41)-Os(4)-P(4)	87.5(15)
C(12)-Os(1)-P(1)	95.9(17)	C(43)-Os(4)-Os(5)	92(2)
C(11)-Os(1)-P(1)	79(2)	C(42)-Os(4)-Os(5)	89.3(15)
C(13)-Os(1)-Os(2)	102.5(16)	C(41)-Os(4)-Os(5)	95.0(15)
C(12)-Os(1)-Os(2)	86.1(18)	P(4)-Os(4)-Os(5)	163.9(7)
C(11)-Os(1)-Os(2)	99(3)	C(43)-Os(4)-Os(6)	152(2)
P(1)-Os(1)-Os(2)	164.3(6)	C(42)-Os(4)-Os(6)	92.1(19)
C(13)-Os(1)-Os(3)	162.2(16)	C(41)-Os(4)-Os(6)	90.8(19)
C(12)-Os(1)-Os(3)	87(2)	P(4)-Os(4)-Os(6)	104.2(7)
C(11)-Os(1)-Os(3)	95(4)	Os(5)-Os(4)-Os(6)	59.98(13)
P(1)-Os(1)-Os(3)	104.7(6)	C(51)-Os(5)-C(54)	101(3)

Os(2)-Os(1)-Os(3)	59.79(10)	C(51)-Os(5)-C(53)	92(2)
C(24)-Os(2)-C(23)	113(3)	C(54)-Os(5)-C(53)	96(4)
C(24)-Os(2)-C(21)	104(2)	C(51)-Os(5)-C(52)	178.5(17)
C(23)-Os(2)-C(21)	91(3)	C(54)-Os(5)-C(52)	80(3)
C(24)-Os(2)-C(22)	75(2)	C(53)-Os(5)-C(52)	89(2)
C(23)-Os(2)-C(22)	93(3)	C(51)-Os(5)-Os(4)	83.8(13)
C(21)-Os(2)-C(22)	175(3)	C(54)-Os(5)-Os(4)	160(3)
C(24)-Os(2)-Os(3)	98.2(14)	C(53)-Os(5)-Os(4)	103(2)
C(23)-Os(2)-Os(3)	149(2)	C(52)-Os(5)-Os(4)	94.8(12)
C(21)-Os(2)-Os(3)	84.4(18)	C(51)-Os(5)-Os(6)	88.5(12)
C(22)-Os(2)-Os(3)	91(2)	C(54)-Os(5)-Os(6)	100(3)
C(24)-Os(2)-Os(1)	157.8(14)	C(53)-Os(5)-Os(6)	163(2)
C(23)-Os(2)-Os(1)	89(2)	C(52)-Os(5)-Os(6)	90.2(12)
C(21)-Os(2)-Os(1)	80.1(17)	Os(4)-Os(5)-Os(6)	60.34(13)
C(22)-Os(2)-Os(1)	98.3(17)	C(62)-Os(6)-C(64)	91(2)
Os(3)-Os(2)-Os(1)	60.22(11)	C(62)-Os(6)-C(63)	94(2)
C(32)-Os(3)-C(34)	87(2)	C(64)-Os(6)-C(63)	90(3)
C(32)-Os(3)-C(33)	73(2)	C(62)-Os(6)-C(61)	170(2)
C(34)-Os(3)-C(33)	111(3)	C(64)-Os(6)-C(61)	96(2)
C(32)-Os(3)-C(31)	169(2)	C(63)-Os(6)-C(61)	94(2)
C(34)-Os(3)-C(31)	85.0(19)	C(62)-Os(6)-Os(5)	83.5(12)
C(33)-Os(3)-C(31)	102(2)	C(64)-Os(6)-Os(5)	174(2)
C(32)-Os(3)-Os(2)	93.0(15)	C(63)-Os(6)-Os(5)	92.4(17)
C(34)-Os(3)-Os(2)	164.3(19)	C(61)-Os(6)-Os(5)	89.2(14)
C(33)-Os(3)-Os(2)	83.7(18)	C(62)-Os(6)-Os(4)	83.9(15)
C(31)-Os(3)-Os(2)	96.4(14)	C(64)-Os(6)-Os(4)	117(2)
C(32)-Os(3)-Os(1)	102.0(15)	C(63)-Os(6)-Os(4)	152.0(17)
C(34)-Os(3)-Os(1)	104.5(19)	C(61)-Os(6)-Os(4)	86.3(17)
C(33)-Os(3)-Os(1)	143.4(18)	Os(5)-Os(6)-Os(4)	59.67(14)
C(31)-Os(3)-Os(1)	87.5(16)	C(2)-P(1)-Os(1)	113(2)
Os(2)-Os(3)-Os(1)	59.99(11)	C(3)-C(2)-P(1)	124(4)
C(43)-Os(4)-C(42)	82(2)	C(2)-C(3)-P(4)	117(4)
C(43)-Os(4)-C(41)	97(3)	C(3)-P(4)-Os(4)	106(2)

Figure 2.3. Crystal Structure of $Os_3(CO)_{11}PPh_2(CH_2)_4PPh_2Os_3(CO)_{11}$

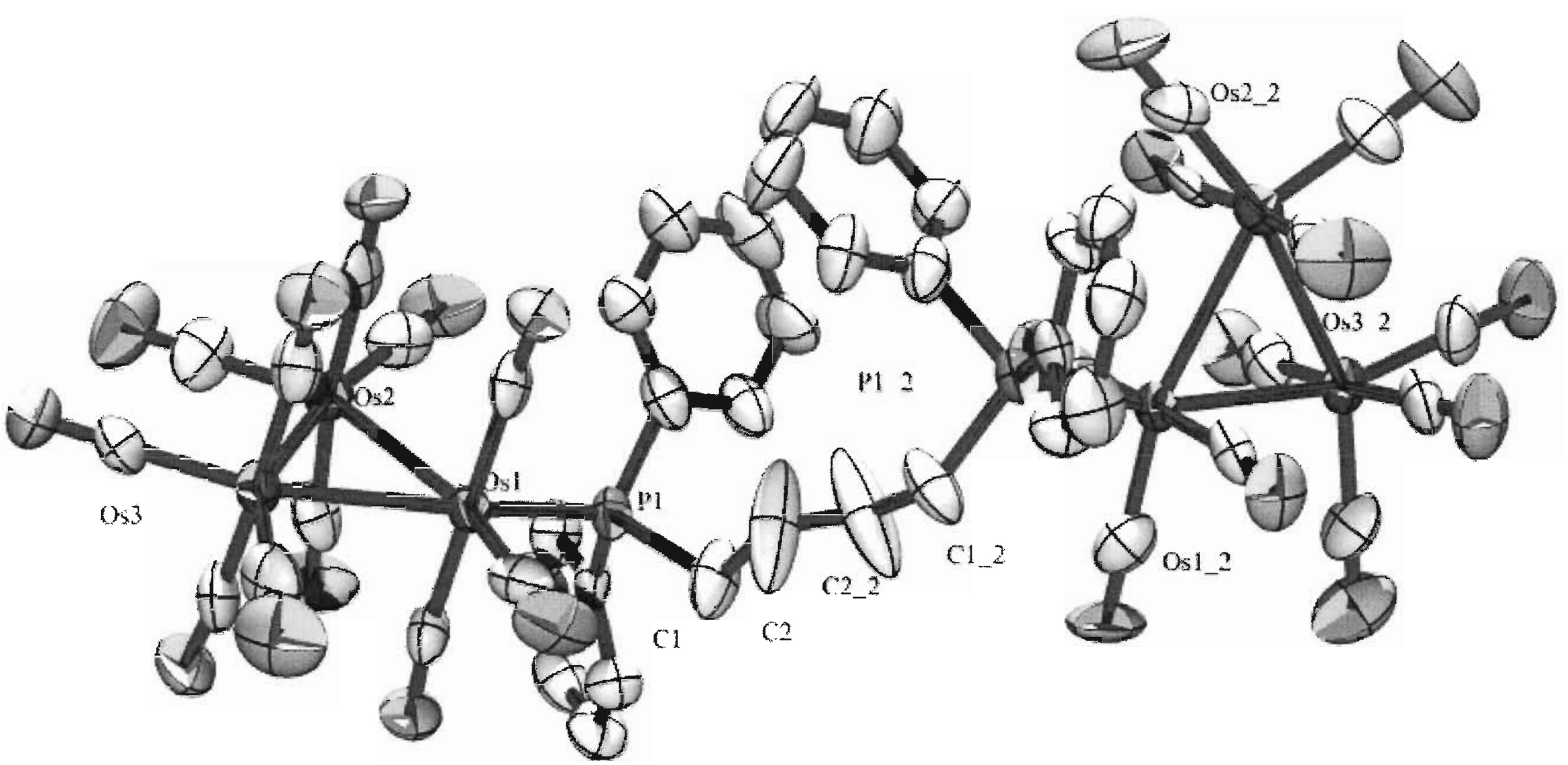

Table 2.7. Selected Bond Lengths and Angles for $Os_3(CO)_{11}PPh_2(CH_2)_4PPh_2Os_3(CO)_{11}$

Bond Lengths (Å)

Os(1)-C(13)	1.90(2)	P(1)-C(1)	1.804(15)
Os(1)-C(12)	1.913(16)	C(1)-C(2)	1.53(2)
Os(1)-C(11)	1.945(17)	C(11)-O(11)	1.137(17)
Os(1)-P(1)	2.345(3)	C(12)-O(12)	1.161(17)
Os(1)-Os(3)	2.8746(7)	C(13)-O(13)	1.12(2)
Os(1)-Os(2)	2.9190(8)	C(21)-O(21)	1.124(19)
Os(2)-C(23)	1.862(18)	C(22)-O(22)	1.127(19)
Os(2)-C(24)	1.89(2)	C(23)-O(23)	1.16(2)
Os(2)-C(22)	1.935(19)	C(24)-O(24)	1.14(2)
Os(2)-C(21)	1.95(2)	C(31)-O(31)	1.116(19)
Os(2)-Os(3)	2.8829(8)	C(32)-O(32)	1.161(18)
Os(3)-C(34)	1.873(17)	C(33)-O(33)	1.13(2)
Os(3)-C(33)	1.91(2)	C(34)-O(34)	1.174(19)
Os(3)-C(32)	1.915(18)	C(2)-C(2)#1	1.22(3)
Os(3)-C(31)	1.97(2)		

Bond Angles (deg)

C(13)-Os(1)-C(12)	91.2(7)	C(21)-Os(2)-Os(3)	87.2(5)
C(13)-Os(1)-C(11)	85.5(6)	C(23)-Os(2)-Os(1)	151.0(6)
C(12)-Os(1)-C(11)	176.2(6)	C(24)-Os(2)-Os(1)	109.3(5)
C(13)-Os(1)-P(1)	98.9(5)	C(22)-Os(2)-Os(1)	86.3(5)
C(12)-Os(1)-P(1)	88.1(4)	C(21)-Os(2)-Os(1)	87.7(4)
C(11)-Os(1)-P(1)	94.2(4)	Os(3)-Os(2)-Os(1)	59.396(18)
C(13)-Os(1)-Os(3)	99.8(5)	C(34)-Os(3)-C(33)	105.1(8)
C(12)-Os(1)-Os(3)	85.8(4)	C(34)-Os(3)-C(32)	87.4(7)
C(11)-Os(1)-Os(3)	93.0(4)	C(33)-Os(3)-C(32)	92.1(8)
P(1)-Os(1)-Os(3)	160.45(9)	C(34)-Os(3)-C(31)	90.7(7)
C(13)-Os(1)-Os(2)	159.0(5)	C(33)-Os(3)-C(31)	91.0(8)
C(12)-Os(1)-Os(2)	91.5(4)	C(32)-Os(3)-C(31)	176.7(7)
C(11)-Os(1)-Os(2)	91.0(4)	C(34)-Os(3)-Os(1)	162.1(6)
P(1)-Os(1)-Os(2)	102.00(9)	C(33)-Os(3)-Os(1)	92.8(5)
Os(3)-Os(1)-Os(2)	59.677(19)	C(32)-Os(3)-Os(1)	92.7(4)
C(23)-Os(2)-C(24)	99.5(8)	C(31)-Os(3)-Os(1)	88.2(4)
C(23)-Os(2)-C(22)	92.0(7)	C(34)-Os(3)-Os(2)	101.3(6)
C(24)-Os(2)-C(22)	88.7(7)	C(33)-Os(3)-Os(2)	153.3(5)
C(23)-Os(2)-C(21)	95.6(7)	C(32)-Os(3)-Os(2)	85.0(5)
C(24)-Os(2)-C(21)	88.7(7)	C(31)-Os(3)-Os(2)	92.7(4)
C(22)-Os(2)-C(21)	172.3(6)	Os(1)-Os(3)-Os(2)	60.927(18)
C(23)-Os(2)-Os(3)	91.9(6)	C(1)-P(1)-Os(1)	112.8(6)
C(24)-Os(2)-Os(3)	168.1(5)	C(2)-C(1)-P(1)	117.7(15)
C(22)-Os(2)-Os(3)	93.9(5)	C(2)#1-C(2)-C(1)	126(2)

C31 on Os3 is leaning towards Os1 but away from Os2, while its *trans* axial carbonyl C32 is leaning towards Os2 but away from Os1. On the phosphine substituted Os1 atom, the axial carbonyl C11 is tilted away from the cluster while its *trans* axial carbonyl C12 is tilted towards Os3 but away from Os2.

2.2.3. $[Os_3(CO)_{10}PPh_2(CH_2)_nPPh_2]_2$

2.2.3.1. Synthesis of $[Os_3(CO)_{10}PPh_2(CH_2)_nPPh_2]_2$

The compound $[Os_3(CO)_{10}PPh_2(CH_2)_4PPh_2]_2$ was prepared by adding small aliquots of a solution of $PPh_2(CH_2)_4PPh_2$ in dichloromethane to a stirring solution $Os_3(CO)_{10}(MeCN)_2$ in dichloromethane. The solvent was removed and the solid purified by column chromatography then recrystallized from CH_2Cl_2/hexanes to produce yellow crystals.

The compound $[Os_3(CO)_{10}PPh_2(CH_2)_6PPh_2]_2$ was prepared in a similar manner but yielded orange crystals.

The compounds were analyzed by infrared spectroscopy in hexanes solution and the absorptions in the carbonyl region for $[Os_3(CO)_{10}PPh_2(CH_2)_4PPh_2]_2$ are as follows: 2084 (w), 2053 (w), 2027 (m), 2014 (m,sh), 2001 (s), 1969 (m), 1954(w) cm^{-1}.

The compound $[Os_3(CO)_{10}PPh_2(CH_2)_6PPh_2]_2$ shows similar absorptions.

Infrared analysis of compound $[Os_3(CO)_{10}PPh_2(CH_2)_nPPh_2]_2$ shows the carbonyl region to have a similar visual profile as that of compounds $Os_3(CO)_{11}PPh_2(CH_2)_nPPh_2$ and $Os_3(CO)_{11}PPh_2(CH_2)_nPPh_2Os_3(CO)_{11}$ with the exception that the peaks are all shifted to lower frequencies. For example, the compound $Os_3(CO)_{11}PPh_2(CH_2)_4PPh_2Os_3(CO)_{11}$

shows a strong band at 2020 cm^{-1}, while the compound $[Os_3(CO)_{10}PPh_2(CH_2)_4PPh_2]_2$ shows a strong band at 2001 cm^{-1}.

This implies that the C-O bonds of the carbonyls on both osmium clusters have been weakened and lengthened, as would result from an increase in π-backdonation from the Os atoms. This is consistent with an increase in electron density on the metal clusters from the additional σ donation of the two extra phosphines.

The compounds $[Os_3(CO)_{10}PPh_2(CH_2)_4PPh_2]_2$ and $[Os_3(CO)_{10}PPh_2(CH_2)_6PPh_2]_2$ were analyzed by mass spectroscopy. Their molecular weights are tabulated in Table 2.8 below.

Table 2.8. Mass Spectroscopic Data of $[Os_3(CO)_{10}PPh_2(CH_2)_nPPh_2]_2$

Compound	n Value	Molecular Weight	
		Calculated	Observed
$[Os_3(CO)_{10}PPh_2(CH_2)_nPPh_2]_2$	4	2554	2554.6
	6	2611	2609.8

The mass spectra of $[Os_3(CO)_{10}PPh_2(CH_2)_4PPh_2]_2$ and $[Os_3(CO)_{10}PPh_2(CH_2)_6PPh_2]_2$ show molecular ions consistent with their molecular formulae. The isotope patterns also agree with the calculated isotopic pattern for these compounds, as shown below for $[Os_3(CO)_{10}PPh_2(CH_2)_6PPh_2]_2$ in Figure 2.4.

The compound $[Os_3(CO)_{10}PPh_2(CH_2)_4PPh_2]_2$ was analyzed by $^{31}P\{^1H\}$ NMR Spectroscopy. The spectrum shows a single doublet resonance at a chemical shift of 33.9 ppm indicating that all four phosphorus atoms in the molecule are equivalent.

The compound $[Os_3(CO)_{10}PPh_2(CH_2)_6PPh_2]_2$ was analyzed by elemental analysis. The observed % carbon was 37.00 and % hydrogen was 2.41, in agreement with the calculated values of 36.81 % carbon and 2.47 % hydrogen for the empirical formula $Os_6P_4C_{80}O_{20}H_{64}$.

Figure 2.4. Comparison of Observed and Calculated Isotopic Patterns of $[Os_3(CO)_{10}PPh_2(CH_2)_6PPh_2]_2$

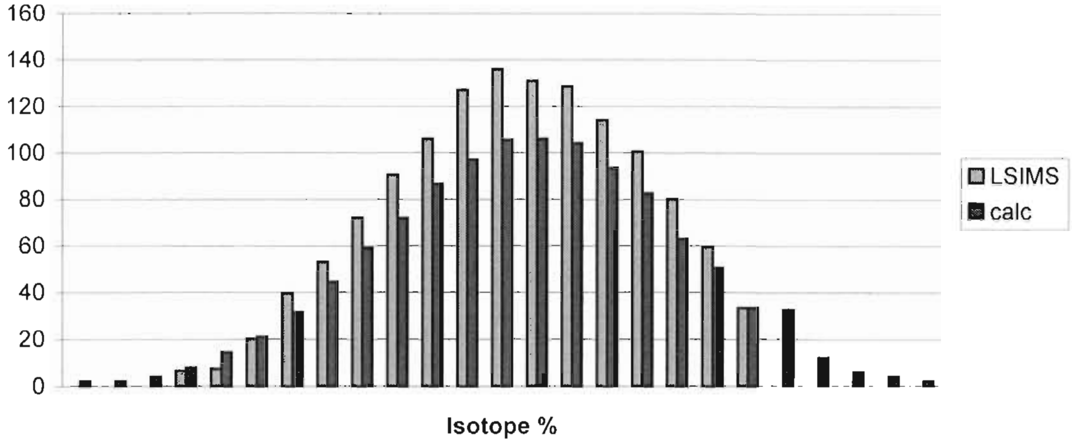

LSIMS	shows the height of each line in mm of the molecular ion peak of $[Os_3(CO)_{10}PPh_2(CH_2)_6PPh_2]_2$ at 2609.8
Calc	shows the height of each line in mm in the calculated isotopic pattern of $[Os_3(CO)_{10}PPh_2(CH_2)_6PPh_2]_2$ generated using the Sheffield Chemputer Website

2.3. Discussion

$Os_3(CO)_{11}PPh_2(CH_2)_nPPh_2$ (n = 1 - 6)

Compound $Os_3(CO)_{11}PPh_2(CH_2)_nPPh_2$ has been previously reported by Deeming *et al.*[15, 18] for n = 1 - 5, however no crystal structures have been presented. The n = 6 analogue is a new compound.

Compound $Os_3(CO)_{11}PPh_2(CH_2)_nPPh_2$ was prepared using two modifications of the procedure reported by Deeming *et al.*. These two modifications resulted in less side-products and result in a simpler and more efficient experimental setup than that presented by Deeming *et al.*.

The compound $Os_3(CO)_{11}(MeCN)$ was slowly added to a stirring solution of excess $PPh_2(CH_2)_nPPh_2$ in dichloromethane over a period of 30 minutes under nitrogen in an ice bath at 0 °C, as shown in Scheme 2.1. The solution was allowed to continue stirring for three hours while slowly warming to room temperature. This procedure differs from that of Deeming *et al.* in that his method required refluxing stoichiometric amounts of both reagents, $PPh_2(CH_2)_nPPh_2$ and $Os_3(CO)_{11}(MeCN)$, in chloroform.

This method represents an improvement over that of Deeming *et al.* according to the following observations. The use of stoichiometrically equivalent amounts of $PPh_2(CH_2)_nPPh_2$ and $Os_3(CO)_{11}(MeCN)$, as indicated in the procedure of Deeming *et al.* produced a large quantity of the side product $Os_3(CO)_{11}PPh_2(CH_2)_nPPh_2Os_3(CO)_{11}$; however, it was found that by using a large excess of $PPh_2(CH_2)_nPPh_2$, the side product $Os_3(CO)_{11}PPh_2(CH_2)_nPPh_2Os_3(CO)_{11}$ could be minimized. This leads to a greater purity in the final product since the compounds $Os_3(CO)_{11}PPh_2(CH_2)_nPPh_2Os_3(CO)_{11}$ and $Os_3(CO)_{11}PPh_2(CH_2)_nPPh_2$ were not easily separated by column chromatography. Furthermore, it was found that heating was unnecessary, as the reaction proceeds to completion at 0 °C, and indeed the low temperature appears to further minimize the formation of compound $Os_3(CO)_{11}PPh_2(CH_2)_nPPh_2Os_3(CO)_{11}$.

Scheme 2.1. Preparation of $Os_3(CO)_{11}PPh_2(CH_2)_nPPh_2$

$$Os_3(CO)_{11}(MeCN) + \text{xs } PPh_2(CH_2)_nPPh_2 \longrightarrow Os_3(CO)_{11}PPh_2(CH_2)_nPPh_2 + Os_3(CO)_{11}PPh_2(CH_2)_nPPh_2Os_3(CO)_{11}$$

Mass spectroscopy of compound $Os_3(CO)_{11}PPh_2(CH_2)_nPPh_2$ (n = 1 - 6) prepared both by Deeming's original procedure and by the modified procedure presented in this thesis, occasionally showed a molecular ion of mass 16 units greater than that of the molecular formula $Os_3(CO)_{11}PPh_2(CH_2)_nPPh_2$.

It is postulated that the uncoordinated phosphine can form a phosphine oxide, either as a result of the mass spectroscopy technique itself, or during the column chromatography step when the compound is inevitably exposed to air. For the purposes of characterizing the compound $Os_3(CO)_{11}PPh_2(CH_2)_nPPh_2$ in this thesis, synthesis of $Os_3(CO)_{11}PPh_2(CH_2)_nPPh_2$ was repeated until the mass spectrum showed no presence of the phosphine oxide.

$Os_3(CO)_{11}PPh_2(CH_2)_nPPh_2Os_3(CO)_{11}$ (n = 2 - 6)

Compound $Os_3(CO)_{11}PPh_2(CH_2)_nPPh_2Os_3(CO)_{11}$ has also been previously reported by Deeming *et al.* for n = 2 – 5,[15, 18] but no crystal structures have been presented. The n = 6 analogue is a new compound. Compound $Os_3(CO)_{11}PPh_2(CH_2)_nPPh_2Os_3(CO)_{11}$ was prepared by a method slightly different from that of Deeming *et al.*, in that it does not involve refluxing stoichiometric amounts of reagents in chloroform. Instead, $PPh_2(CH_2)_nPPh_2$ was added dropwise to a stirring solution of excess $Os_3(CO)_{11}(MeCN)$ in dichloromethane at room temperature over a period of 30 minutes.

Scheme 2.2. Preparation of $Os_3(CO)_{11}PPh_2(CH_2)_nPPh_2Os_3(CO)_{11}$

$$\text{xs } 2Os_3(CO)_{11}(MeCN) + PPh_2(CH_2)_nPPh_2 \longrightarrow Os_3(CO)_{11}PPh_2(CH_2)_nPPh_2Os_3(CO)_{11}$$

By this method, compound $Os_3(CO)_{11}PPh_2(CH_2)_nPPh_2Os_3(CO)_{11}$ was produced in high yield with only trace amounts of the side product $Os_3(CO)_{11}PPh_2(CH_2)_nPPh_2$. The excess $Os_3(CO)_{11}(MeCN)$ was easily removed by column chromatography. Compound $Os_3(CO)_{11}PPh_2(CH_2)_nPPh_2Os_3(CO)_{11}$ formed yellow crystals from a slow infusion of hexanes into dichloromethane, which were stable in air for several weeks.

$[Os_3(CO)_{10}PPh_2(CH_2)_nPPh_2]_2$ (n = 4, 6)

Compound $[Os_3(CO)_{10}PPh_2(CH_2)_nPPh_2]_2$ was prepared by slow addition of $PPh_2(CH_2)_nPPh_2$ to $Os_3(CO)_{10}(MeCN)_2$ in dichloromethane at room temperature, according to the following scheme.

Scheme 2.3. Preparation of $[Os_3(CO)_{10}PPh_2(CH_2)_nPPh_2]_2$

$$PPh_2(CH_2)_nPPh_2 + Os_3(CO)_{10}(MeCN)_2 \longrightarrow [Os_3(CO)_{10}PPh_2(CH_2)_nPPh_2]_2 + Os_3(CO)_{10}(\mu\text{-}PPh_2(CH_2)_nPPh_2)$$

Deeming *et al.*[13] performed a similar reaction in refluxing chloroform and found the only product to be $Os_3(CO)_{10}(\mu\text{-}PPh_2(CH_2)_nPPh_2)$, although they did report a trace amount of an uncharacterized compound, which may have been $[Os_3(CO)_{10}PPh_2(CH_2)_nPPh_2]_2$. These milder reaction conditions, while still producing $Os_3(CO)_{10}(\mu\text{-}PPh_2(CH_2)_nPPh_2)$ as the major product, produces compound $[Os_3(CO)_{10}PPh_2(CH_2)_nPPh_2]_2$ in approximately 20% yield.

The proposed structure of $[Os_3(CO)_{10}PPh_2(CH_2)_nPPh_2]_2$ is a double bridged system shown in the figure below.

Figure 2.5. Proposed Structure of $[Os_3(CO)_{10}PPh_2(CH_2)_nPPh_2]_2$

* Carbonyls are omitted

* $PPh_2(CH_2)_nPPh_2$ is represented by

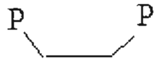

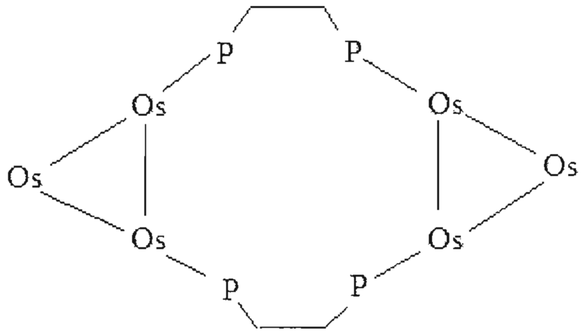

This type of structure, when compared to that of compound $Os_3(CO)_{11}PPh_2(CH_2)_nPPh_2Os_3(CO)_{11}$, has two extra P→Os dative sigma bonds which increases the electron density on both of the clusters. This in turn increases the amount of backdonation from the filled *d* shell of the osmium atoms to the empty π* orbital of the carbonyl ligand, thus lowering the bond order of the C-O bond and decreasing its vibrational energy.

The results of the infrared analysis are consistent with the type of dimer structure for compound $[Os_3(CO)_{10}PPh_2(CH_2)_nPPh_2]_2$ in which both phosphines of each of the bidentate $PPh_2(CH_2)_nPPh_2$ groups are bridged between adjacent osmium atoms on each of the osmium clusters.

Further evidence for the proposed structure as shown in Figure 2.5. is provided by the $^{31}P\{^1H\}$ NMR spectrum of $[Os_3(CO)_{10}PPh_2(CH_2)_4PPh_2]_2$ which shows one resonance at a chemical shift of 33.9 ppm, indicating that all four P atoms in the molecule are equivalent.

The other possible structure that would agree with the spectroscopic evidence is that in which the two bidentate phosphines bridge across a single osmium atom on each triosmium cluster.

This structure however is rejected due to the following reason. In the starting material, $Os_3(CO)_{10}(MeCN)_2$, the two labile acetonitrile groups are known to bond on adjacent osmium atoms in the axial positions. In general, substitution by two phosphines to form $Os_3(CO)_{10}(PR_3)_2$ involves coordination of the phosphines in the equatorial positions of the two adjacent osmium atoms, migration of the carbonyls to the axial positions, and release of two molecules of acetonitrile. In this way, the compound $Os_3(CO)_{10}(PR_3)_2$ results in a structure in which the two PR_3 groups exist in equatorial positions on two adjacent osmium atoms of the triosmium cluster. Knowing this, it does not seem likely that the compound $[Os_3(CO)_{10}PPh_2(CH_2)_nPPh_2]_2$ has a structure in which the two bidentate phosphines bridge across a single osmium atom on each triosmium cluster.

2.4. Conclusion

X-ray crystal structures of $Os_3(CO)_{11}PPh_2(CH_2)_nPPh_2$ (n = 2) and $Os_3(CO)_{11}PPh_2(CH_2)_nPPh_2Os_3(CO)_{11}$ (n = 2, 4) have been presented. The structures are consistent with that postulated by Deeming *et al.* in the original publication of their synthesis in 1987.[15]

The synthesis and characterization of a new osmium derivative $[Os_3(CO)_{10}PPh_2(CH_2)_nPPh_2]_2$ (n = 4, 6) has been described. Spectroscopic evidence suggests the structure to be a dimer in which each $PPh_2(CH_2)_nPPh_2$ unit forms a bridge between triosmium clusters as a result of each phosphine coordinating to a different osmium atom on each triosmium cluster.

2.5. Experimental

2.5.1. General Methods

Unless otherwise stated, all starting materials and products in this chapter were handled under an inert atmosphere of nitrogen using standard Schlenk techniques. The masses and volumes listed in the preparation of compounds are approximate.

2.5.2. Materials

Hexanes was refluxed over potassium, distilled and stored under nitrogen. Acetonitrile and dichloromethane were refluxed over CaH_2, distilled and stored under nitrogen. $PPh_2(CH_2)_nPPh_2$ (n = 1 - 4) were obtained commercially from Strem and $PPh_2(CH_2)_nPPh_2$ (n = 5, 6) from Aldrich Chemicals Company. OsO_4 was obtained commercially from Pressure Chemical Company and $Os_3(CO)_{12}$ was prepared by a literature method.[9]

2.5.3. Instrumentation

Infrared Spectra were recorded on a Bomem MB-Series spectrophotometer; samples were contained in cells with NaCl windows. $^{31}P\{^1H\}$ NMR were recorded by Mr. Colin Zhang at Simon Fraser University on either a Brucker Avance 600 NMR instrument at an operating frequency of 242.925 MHz or a Varian Mercury 400 NMR instrument at an operating frequency of 161.965 MHz. Elemental analyses were performed by M. K. Yang at the Microanalytical Laboratory at Simon Fraser University. Mass Spectroscopy (LSIMS) was performed by David McGillivray at the University of Victoria. X-ray crystallography was performed by Dr. Michael Jennings at the University of Western Ontario.

2.5.4. Preparation of Compounds

Preparation of $Os_3(CO)_{11}PPh_2(CH_2)_4PPh_2$

To a solution of excess $PPh_2(CH_2)_4PPh_2$ (94 mg, 0.22 mmol) in dichloromethane (30 mL) was added in small aliquots $Os_3(CO)_{11}(MeCN)$ (100 mg, 0.11 mmol) in dichloromethane (10 mL) at 0 °C over 30 minutes. The reaction was slowly warmed to room temperature while stirring for 3 hours during which time the yellow solution turned orange. The solution was evaporated to dryness and the solid subjected to chromatography on a silica gel column. Elution with hexane / CH_2Cl_2 (80/20 by volume) gave a yellow band of $Os_3(CO)_{11}PPh_2(CH_2)_4PPh_2Os_3(CO)_{11}$ immediately followed by an orange band of the desired product (yield ~ 60%). $Os_3(CO)_{11}PPh_2(CH_2)_4PPh_2$ was recrystallized on slow cooling in hexanes to give orange crystals. The compounds $Os_3(CO)_{11}PPh_2(CH_2)_nPPh_2$ (n = 1 - 3, 5 - 6) were prepared in a similar manner. $Os_3(CO)_{11}PPh_2CH_2PPh_2$: IR hexanes υ(CO) 2107 (w), 2054 (m), 2035 (m), 2019 (s), 2001 (w), 1990 (m), 1981 (w), 1976 (w), 1969 (w), 1954 (w) cm^{-1}; MS (LSIMS) *m/z* 1263.8 (Calcd = 1264 (100%)). $Os_3(CO)_{11}PPh_2(CH_2)_2PPh_2$: IR hexanes υ(CO) 2107 (w), 2054 (m), 2035 (m), 2019 (s), 2001 (w), 1990 (m), 1981 (w), 1976 (w), 1969 (w), 1954 (w) cm^{-1}; MS (LSIMS) *m/z* 1275.8 (Calcd = 1278 (100%)) Elemental Analysis Calculated for $Os_3P_2C_{37}O_{11}H_{24}$: 34.79 %C; 1.89 %H. Observed: 34.66 %C; 1.81 %H. $Os_3(CO)_{11}PPh_2(CH_2)_3PPh_2$: IR hexanes υ(CO) 2107 (w), 2054 (m), 2035 (m), 2019 (s), 2001 (w), 1990 (m), 1981 (w,b) cm^{-1}. $Os_3(CO)_{11}PPh_2(CH_2)_4PPh_2$: IR hexanes υ(CO) 2108 (w), 2055 (m), 2035 (m), 2020 (s), 2002 (w), 1991 (m), 1981 (w,b) cm^{-1}; MS (LSIMS) *m/z* 1304.7 (Calcd = 1306 (100%)). $Os_3(CO)_{11}PPh_2(CH_2)_5PPh_2$: IR hexanes υ(CO) 2107 (w), 2054 (m), 2034 (m), 2019 (s), 2001 (w), 1990 (m), 1973 (w,b), 1958 (w,b) cm^{-1}; MS (LSIMS) *m/z* 1319.7 (Calcd = 1320 (100%)). $Os_3(CO)_{11}PPh_2(CH_2)_6PPh_2$: IR hexanes υ(CO) 2107 (w), 2054 (m), 2034 (m), 2019 (s), 2001 (w), 1990 (m), 1978 (w,b) cm^{-1}.

Preparation of $Os_3(CO)_{11}PPh_2(CH_2)_4PPh_2Os_3(CO)_{11}$

To a solution of excess $Os_3(CO)_{11}(MeCN)$ (200 mg, 0.22 mmol) in dichloromethane (10 mL) was added in small aliquots $PPh_2(CH_2)_4PPh_2$ (23 mg, 0.055 mmol) in dichloromethane (5 mL) at room temperature. The reaction was stirred overnight during which time the yellow solution turned deeper yellow. The solution was evaporated to dryness and the solid subjected to chromatography on a silica gel column. Elution with hexane / CH_2Cl_2 (80/20 by volume) gave a yellow band of the desired product immediately followed by a faint orange band of $Os_3(CO)_{11}PPh_2(CH_2)_4PPh_2$. The compound $Os_3(CO)_{11}PPh_2(CH_2)_4PPh_2Os_3(CO)_{11}$ (yield ~ 80%) was recrystallized from hexane / CH_2Cl_2 to give yellow crystals. The compounds $Os_3(CO)_{11}PPh_2(CH_2)_nPPh_2Os_3(CO)_{11}$ (n = 2 - 3, 5 - 6) were prepared by a similar method. $Os_3(CO)_{11}PPh_2CH_2PPh_2Os_3(CO)_{11}$ could not be prepared by this method. $Os_3(CO)_{11}PPh_2(CH_2)_2PPh_2Os_3(CO)_{11}$: IR hexanes υ(CO) 2107 (w), 2055 (m), 2035 (m), 2020 (s), 2004 (w), 1991 (m), 1979 (w,b) cm^{-1}; MS (LSIMS) *m/z* 2155.1 (Calcd = 2156 (100%)); ^{31}P NMR ($CDCl_3$) δ −8.7 (s) ppm; Elemental Analysis Calculated for

$Os_6P_2C_{48}O_{22}H_{24}$: 26.79 %C; 1.12 %H. Observed: 26.63 %C; 1.24 %H. $Os_3(CO)_{11}PPh_2(CH_2)_3PPh_2Os_3(CO)_{11}$: IR hexanes υ(CO) 2106 (w), 2055 (m), 2035 (m), 2019 (s), 2002 (w), 1991 (m), 1982 (w), 1965(w) cm^{-1}; MS (LSIMS) *m/z* 2171.7 (Calcd = 2170 (100%)); $^{31}P\{^1H\}$ NMR ($CDCl_3$) δ –8.6 (s) ppm;. $Os_3(CO)_{11}PPh_2(CH_2)_4PPh_2Os_3(CO)_{11}$: IR hexanes υ(CO) 2108 (w), 2055 (m), 2035 (m), 2020 (s), 2002 (w), 1991 (m), 1982 (w,b) cm^{-1}; MS (LSIMS) *m/z* 2184.4 (Calcd = 2184 (100%)); $^{31}P\{^1H\}$ NMR ($CDCl_3$) δ –8.3 (s) ppm; Elemental Analysis Calculated for $Os_6P_2C_{50}O_{22}H_{28}$: 27.50 %C; 1.29 %H. Observed: 27.86 %C; 1.38 %H. $Os_3(CO)_{11}PPh_2(CH_2)_5PPh_2Os_3(CO)_{11}$: IR hexanes υ(CO) 2107 (w), 2055 (m), 2034 (m), 2019 (s), 2002 (w), 1991 (m), 1980 (w,b)cm^{-1}; MS (LSIMS) *m/z* 2197.6 (Calcd = 2198 (100%)); $^{31}P\{^1H\}$ NMR ($CDCl_3$) δ –7.3 (s) ppm; Elemental Analysis Calculated for $Os_6P_2C_{51}O_{22}H_{30}$: 27.87 %C; 1.38 %H. Observed: 27.79 %C; 1.46 %H. $Os_3(CO)_{11}PPh_2(CH_2)_6PPh_2Os_3(CO)_{11}$: IR hexanes υ(CO) 2107 (w), 2055 (m), 2035 (m), 2019 (s), 2002 (w), 1990 (m), 1979 (w,b) cm^{-1}; MS (LSIMS) *m/z* 2213.5 (Calcd = 2212 (100%)); $^{31}P\{^1H\}$ NMR ($CDCl_3$) δ –8.2 (s) ppm; Elemental Analysis Calculated for $Os_6P_2C_{52}O_{22}H_{32}$: 28.23 %C; 1.46 %H. Observed: 28.46 %C; 1.60 %H.

Preparation of $[Os_3(CO)_{10}PPh_2(CH_2)_4PPh_2]_2$

To a solution of $Os_3(CO)_{10}(MeCN)_2$ (200mg, 0.21 mmol) in dichloromethane (10 mL) was added in small aliquots $PPh_2(CH_2)_4PPh_2$ (91 mg, 0.21 mmol) in dichloromethane (5 mL) over a period of 20 minutes. During this time the yellow solution turned orange-red. The reaction was stirred for two days with no further colour change. The solution was evaporated to dryness and the solid subjected to chromatography on a silica gel column. Elution with hexane / CH_2Cl_2 (80 / 20 by volume) gave a yellow band of $Os_3(CO)_{11}PPh_2(CH_2)_4PPh_2Os_3(CO)_{11}$, (70 / 30 by volume) an orange-red band of $Os_3(CO)_{10}PPh_2(CH_2)_4PPh_2$, (65 / 35 by volume) a pale yellow band of an unknown compound, (60 / 40 by volume) a yellow band of an unknown compound, and (50 / 50 by volume) an orange-red band of the desired compound $[Os_3(CO)_{10}PPh_2(CH_2)_4PPh_2]_2$ (yield ~ 10 %). The compound $[Os_3(CO)_{10}PPh_2(CH_2)_4PPh_2]_2$ was recrystallized from hexanes / CH_2Cl_2 to give yellow crystals. Alternatively, the compound was also recrystallized from toluene / hexanes and chlorobenzene / hexanes to give orange crystals. $[Os_3(CO)_{10}PPh_2(CH_2)_4PPh_2]_2$: IR hexanes υ(CO) 2084 (w), 2053 (w), 2027 (m), 2014 (m,sh), 2001 (s), 1969 (m), 1954(w) cm^{-1}; MS (LSIMS) *m/z* 2554.6 (Calcd = 2554 (100%)); $^{31}P\{^1H\}$ NMR ($CDCl_3$) δ 33.9 (d) ppm. $[Os_3(CO)_{10}PPh_2(CH_2)_6PPh_2]_2$: IR hexanes υ(CO) 2084 (w), 2053 (w), 2027 (m), 2014 (m,sh), 2000 (s), 1967 (m), 1953(w) cm^{-1}; MS (LSIMS) *m/z* 2609.8 (Calcd = 2611 (100%)); Elemental Analysis Calculated for $Os_6P_4C_{80}O_{20}H_{64}$: 36.81 %C; 2.47 %H. Observed: 37.00 %C; 2.41 %H.

CHAPTER 3

THE GROUP 6 DERIVATIVES OF $Os_3(CO)_{11}PPh_2(CH_2)_nPPh_2$

3.1. Introduction

In this chapter is described the use of a bidentate phosphine to link a triosmium cluster to a group 6 moiety. This has been accomplished in the past by several different methods.

In 2004, the group of Yeh *et al.*[22] described the preparation of $Os_3(CO)_{10}[(\mu,\eta^2\text{-}Ph_2PC{\equiv}CPPh_2)W(\eta^2\text{-}PhC{\equiv}CPh)_3]_2$. They found that the rigidity of the $-C{\equiv}C-$ unit acts to force the ligand to bond between two different metal centres, thus being very useful in this type of application.

In 1991, the group of Tseng *et al.*[23] reported the synthesis and X-ray crystal structure of $Cp(CO)_2[P(OMe)_3]W(\mu,\eta^1,\eta^2\text{-}CH_2CH{=}CH)Os_3(CO)_{10}H$ from the monophosphite-substituted tungsten allenyl carbonyl complex $Cp(CO)_2[P(OMe)_3]WCH_2C{\equiv}CH$ with $H_2Os_3(CO)_{10}$.

In 1984 Adams *et al.*[24] reported the preparation of $Os_3(CO)_9(\mu_3{-}S)(\mu_4{-}S)[W(CO)_5]$ in which the tungsten moiety is bound to the triosmium cluster via a triply bridged sulfido ligand. This type of ligand coordinates through donation of a lone pair of electrons to other unsaturated metal centres.

The goal of this chapter is to coordinate various transition metal accepting groups to the dangling phosphine of $Os_3(CO)_{11}PPh_2(CH_2)_nPPh_2$ including the group 6 moieties $Cr(CO)_5$, $Mo(CO)_5$, and $W(CO)_5$, while simultaneously varying the carbon chain length from one to six carbons in the bidentate phosphine.

3.2. Results

3.2.1. $Os_3(CO)_{11}PPh_2(CH_2)_nPPh_2Cr(CO)_5$

3.2.1.1. Synthesis of $Os_3(CO)_{11}PPh_2(CH_2)_nPPh_2Cr(CO)_5$

The compound $Os_3(CO)_{11}PPh_2(CH_2)_2PPh_2Cr(CO)_5$ was prepared by cooling a solution of excess $Cr(CO)_5THF$ in THF to –196 °C and adding a solution of $Os_3(CO)_{11}PPh_2(CH_2)_2PPh_2$ in dichloromethane. The tube was stored in the freezer for 1 to 6 days and then the solvent was removed. The solid was purified by column chromatography then recrystallized from hexane / CH_2Cl_2 to give orange crystals.

The compounds $Os_3(CO)_{11}PPh_2(CH_2)_nPPh_2Cr(CO)_5$ ($n = 1$ and 3 - 6) were prepared in a similar manner. In each case the result was orange crystals.

The compounds were analyzed by infrared spectroscopy in hexanes solution. The absorptions in the carbonyl region for $Os_3(CO)_{11}PPh_2(CH_2)_2PPh_2Cr(CO)_5$ are as follows: 2108 (m), 2064 (m), 2056 (s), 2034 (m), 2020 (s), 2003 (w), 1991 (m), 1983 (w,b), 1954 (m), 1939 (s) cm^{-1}.

The compounds $Os_3(CO)_{11}PPh_2(CH_2)_nPPh_2Cr(CO)_5$ ($n = 1$ and 3 - 6) show similar absorptions and, as expected, the absorptions do not vary with the length of the carbon chain.

The compounds $Os_3(CO)_{11}PPh_2(CH_2)_nPPh_2Cr(CO)_5$ ($n = 1$ - 6) were analyzed by mass spectroscopy. Their molecular weights are tabulated in Table 3.1 below.

Table 3.1. Mass Spectroscopy Data of $Os_3(CO)_{11}PPh_2(CH_2)_nPPh_2Cr(CO)_5$

Compound	n Value	Molecular Weight	
		Calculated	Observed
$Os_3(CO)_{11}PPh_2(CH_2)_nPPh_2M(CO)_5$ (M=Cr)	1	1456	1452.6
	2	1470	1467.5
	3	1484	1483.6
	4	1498	1497.6
	5	1512	1511.9
	6	1526	1525.8

In some cases there are slight variations between the calculated molecular weight and the observed molecular weight, particularly in compounds $Os_3(CO)_{11}PPh_2CH_2PPh_2Cr(CO)_5$ and $Os_3(CO)_{11}PPh_2(CH_2)_2PPh_2Cr(CO)_5$. The reason for this could be variability in the technique used to generate the spectra.[20] Notwithstanding these slight deviations, the mass spectra of $Os_3(CO)_{11}PPh_2(CH_2)_nPPh_2Cr(CO)_5$ show molecular ions consistent with their molecular formulae.

The compounds $Os_3(CO)_{11}PPh_2(CH_2)_nPPh_2Cr(CO)_5$ (n = 1 - 6) were analyzed by $^{31}P\{^1H\}$ NMR Spectroscopy. Their chemical shifts are tabulated in Table 3.2 below.

Table 3.2. $^{31}P\{^1H\}$ NMR Spectroscopy Data of $Os_3(CO)_{11}PPh_2(CH_2)_nPPh_2Cr(CO)_5$

Compound	n Value	^{31}P NMR Resonances	
$Os_3(CO)_{11}PPh_2(CH_2)_nPPh_2M(CO)_5$ (M=Cr)	1	-7.5 (d)	57.6 (d)
	2	-7.8 (d)	50.6 (d)
	3	-8.8 (s)	47.7 (s)
	4	-9.0 (s)	46.4 (s)
	5	-7.1 (s)	47.2 (s)
	6	-8.8 (s)	46.2 (s)

The compounds $Os_3(CO)_{11}PPh_2(CH_2)_nPPh_2Cr(CO)_5$ (n = 1 - 6) show two resonance signals indicating that there are two distinct phosphorus atoms in the molecule. Phosphorus-phosphorus coupling is observed in $Os_3(CO)_{11}PPh_2CH_2PPh_2Cr(CO)_5$ and $Os_3(CO)_{11}PPh_2(CH_2)_2PPh_2Cr(CO)_5$ but not in the longer carbon chain molecules (n = 4 - 6) as is expected. The chemical shift values do not vary significantly with the carbon chain length.

The compounds $Os_3(CO)_{11}PPh_2CH_2PPh_2Cr(CO)_5$ (n = 2, 4, 5) were analyzed by elemental analysis. The results of elemental analysis are tabulated below in Table 3.3.

Table 3.3. Elemental Analysis Data of $Os_3(CO)_{11}PPh_2(CH_2)_nPPh_2Cr(CO)_5$

Compound	**n Value**	**Elemental Analysis**			
		Calculated		**Observed**	
		% C	**% H**	**% C**	**% H**
$Os_3(CO)_{11}PPh_2(CH_2)_nPPh_2M(CO)_5$ (M=Cr)	2	34.33	1.65	34.17	1.61
	4	35.29	1.88	35.55	1.96
	5	35.76	2.00	35.55	2.11

The observed % carbon and % hydrogen agree within uncertainty to the calculated values for the empirical formula of the compounds $Os_3(CO)_{11}PPh_2CH_2PPh_2Cr(CO)_5$ (n = 2, 4, 5).

3.2.2. $Os_3(CO)_{11}PPh_2CH_2PPh_2Mo(CO)_5$

3.2.2.1. Synthesis of $Os_3(CO)_{11}PPh_2(CH_2)_nPPh_2Mo(CO)_5$

The compound $Os_3(CO)_{11}PPh_2(CH_2)_2PPh_2Mo(CO)_5$ was prepared by cooling a solution of excess $Mo(CO)_5THF$ in THF to –196 °C and adding a solution of $Os_3(CO)_{11}PPh_2(CH_2)_2PPh_2$ in dichloromethane. The tube was stored in the freezer for 1 to 6 days and then the solvent was removed. The solid was purified by column chromatography then recrystallized from hexane / CH_2Cl_2 to give yellow crystals.

The compounds $Os_3(CO)_{11}PPh_2(CH_2)_nPPh_2Mo(CO)_5$ (n = 1, 3 - 6) were prepared in a similar manner, however, compounds $Os_3(CO)_{11}PPh_2(CH_2)_nPPh_2Mo(CO)_5$ (n = 1, 3-6) failed to crystallize but yielded a yellow powder.

The compounds were analyzed by infrared spectroscopy in hexanes solution. The absorptions in the carbonyl region for $Os_3(CO)_{11}PPh_2(CH_2)_2PPh_2Mo(CO)_5$ are as follows: 2108 (w), 2073 (m), 2056 (m), 2034 (m), 2021 (s), 2003 (w), 1992 (m), 1980 (w,b), 1952 (m), 1939 (s) cm^{-1}.

The compounds $Os_3(CO)_{11}PPh_2(CH_2)_nPPh_2Mo(CO)_5$ (n = 1 and 3 - 6) show similar absorptions and, as expected, the absorptions do not vary with the length of the carbon chain.

The compounds $Os_3(CO)_{11}PPh_2(CH_2)_nPPh_2Mo(CO)_5$ (n = 1 - 6) were analyzed by mass spectroscopy. Their molecular weights are tabulated in Table 3.4 below.

Table 3.4. Mass Spectroscopic Data of $Os_3(CO)_{11}PPh_2(CH_2)_nPPh_2Mo(CO)_5$

Compound	**n Value**	**Molecular Weight**	
		Calculated	**Observed**
$Os_3(CO)_{11}PPh_2(CH_2)_nPPh_2Mo(CO)_5$	1	1500	1497.5
	2	1514	1511.7
	3	1528	1525.5
	4	1542	1540.6
	5	1556	1556.6
	6	1570	1569.7

In some cases there are slight variations between the calculated molecular weight and the observed molecular weight, particularly in compounds

$Os_3(CO)_{11}PPh_2CH_2PPh_2Mo(CO)_5$, $Os_3(CO)_{11}PPh_2(CH_2)_2PPh_2Mo(CO)_5$, and $Os_3(CO)_{11}PPh_2(CH_2)_3PPh_2Mo(CO)_5$. As explained in chapter 2, this apparent inconsistency can be attributed to variability in the technique used to generate the spectra and is not unusual.[20] Notwithstanding these slight deviations, the mass spectra of $Os_3(CO)_{11}PPh_2(CH_2)_nPPh_2Mo(CO)_5$ show molecular ions consistent with their molecular formulae.

The compounds $Os_3(CO)_{11}PPh_2(CH_2)_nPPh_2Mo(CO)_5$ (n = 2 - 6) were analyzed by $^{31}P\{^1H\}$ NMR Spectroscopy. Their chemical shifts are tabulated in Table 3.5 below. $Os_3(CO)_{11}PPh_2CH_2PPh_2Mo(CO)_5$ was not analyzed by $^{31}P\{^1H\}$ NMR because a quantity sufficient for analysis could not be prepared.

Table 3.5. $^{31}P\{^1H\}$ NMR Spectroscopy Data of $Os_3(CO)_{11}PPh_2(CH_2)_nPPh_2Mo(CO)_5$

Compound	n Value	^{31}P NMR Resonances	
	2	-7.8 (d)	31.2 (d)
	3	-9.6 (s)	27.8 (s)
	4	-8.8 (s)	27.9 (s)
	5	-7.1 (s)	28.8 (s)
	6	-8.6 (s)	27.9 (s)

The compounds $Os_3(CO)_{11}PPh_2(CH_2)_nPPh_2Mo(CO)_5$ (n = 2 - 6) show two resonance signals indicating that there are two distinct phosphorus atoms in the molecule. Phosphorus-phosphorus coupling is observed in $Os_3(CO)_{11}PPh_2(CH_2)_2PPh_2Mo(CO)_5$ but not in the longer carbon chain molecules (n = 3 - 6) as is expected. The chemical shift values do not vary significantly with the carbon chain length.

The compound $Os_3(CO)_{11}PPh_2(CH_2)_2PPh_2Mo(CO)_5$ was analyzed by elemental analysis. The observed % carbon was 33.55 and % hydrogen was 1.79, in agreement with the calculated values of 33.34 % carbon and 1.60 % hydrogen for the empirical formula $Os_3MoP_2C_{42}O_{16}H_{24}$.

3.2.3. $Os_3(CO)_{11}PPh_2CH_2PPh_2W(CO)_5$

3.2.3.1. Synthesis of $Os_3(CO)_{11}PPh_2(CH_2)_nPPh_2W(CO)_5$

The compound $Os_3(CO)_{11}PPh_2(CH_2)_2PPh_2W(CO)_5$ was prepared by cooling a solution of excess $W(CO)_5THF$ in THF to –196 °C and adding a solution of $Os_3(CO)_{11}PPh_2(CH_2)_2PPh_2$ in dichloromethane. The tube was stored in the freezer for 1 to 6 days and then the solvent was removed. The solid was purified by column chromatography and then recrystallized from hexane / CH_2Cl_2 to give orange crystals.

The compounds $Os_3(CO)_{11}PPh_2(CH_2)_nPPh_2W(CO)_5$ (n = 1 and 3 - 6) were prepared in a similar manner. In each case the result was orange crystals.

The compounds were analyzed by infrared spectroscopy in hexanes solution. The absorptions in the carbonyl region for $Os_3(CO)_{11}PPh_2(CH_2)_2PPh_2W(CO)_5$ are as follows: 2108 (w), 2073 (w), 2056 (m), 2034 (m), 2021 (s), 2003 (w), 1992 (m), 1980 (w,b), 1952 (m), 1939 (s) cm^{-1}.

The compounds $Os_3(CO)_{11}PPh_2(CH_2)_nPPh_2W(CO)_5$ (n = 1 and 3 - 6) show similar absorptions and, as expected, the absorptions do not vary with the length of the carbon chain.

The compounds $Os_3(CO)_{11}PPh_2(CH_2)_nPPh_2W(CO)_5$ (n = 1 - 6) were analyzed by mass spectroscopy. Their molecular weights are tabulated in Table 3.6 below.

Table 3.6. Mass Spectroscopic Data for $Os_3(CO)_{11}PPh_2(CH_2)_nPPh_2W(CO)_5$

Compound	n Value	Molecular Weight	
		Calculated	Observed
$Os_3(CO)_{11}PPh_2(CH_2)_nPPh_2W(CO)_5$	1	1588	1586.5
	2	1602	1599.7
	3	1616	1615.6
	4	1630	1629.6
	5	1644	1643.8
	6	1658	1657.8

Although there are some slight deviations due to the variability in the technique used to generate the spectra,[20] the mass spectra of $Os_3(CO)_{11}PPh_2(CH_2)_nPPh_2W(CO)_5$ show molecular ions consistent with their molecular formulae. The isotope patterns also agree with the calculated isotopic pattern for these compounds, as shown below for $Os_3(CO)_{11}PPh_2(CH_2)_5PPh_2W(CO)_5$ in Figure 3.1.

The compounds $Os_3(CO)_{11}PPh_2(CH_2)_nPPh_2W(CO)_5$ (n = 1 - 6) were analyzed by $^{31}P\{^1H\}$ NMR Spectroscopy. Their chemical shifts are tabulated in Table 3.7 below.

Table 3.7. $^{31}P\{^1H\}$ NMR Spectroscopy Data of $Os_3(CO)_{11}PPh_2(CH_2)_nPPh_2W(CO)_5$

Compound	n Value	^{31}P NMR Resonances	
$Os_3(CO)_{11}PPh_2(CH_2)_nPPh_2W(CO)_5$	1	-7.9 (d)	14.8 (d)
	2	-8.2 (d)	12.2 (d)
	3	-8.7 (s)	10.2 (s)
	4	-8.9 (s)	9.5 (s)
	5	-8.3 (s)	9.8 (s)
	6	-8.6 (s)	9.8 (s)

The compounds $Os_3(CO)_{11}PPh_2(CH_2)_nPPh_2W(CO)_5$ (n = 1 - 6) show two resonance signals indicating that there are two distinct phosphorus atoms in the molecule.

Figure 3.1. Comparison of Observed and Calculated Isotopic Patterns of $Os_3(CO)_{11}PPh_2(CH_2)_5PPh_2W(CO)_5$

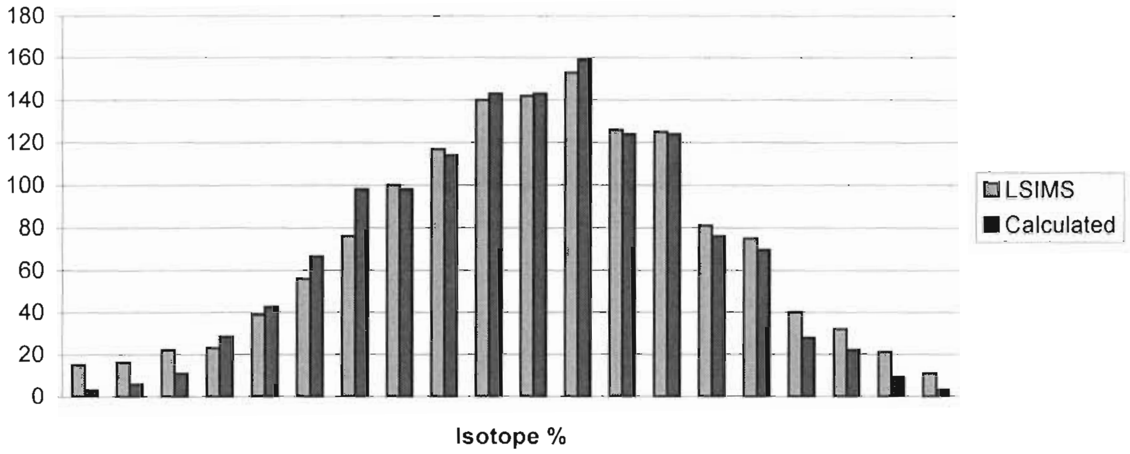

LSIMS	shows the height of the lines in mm of the molecular ion peak of $Os_3(CO)_{11}PPh_2(CH_2)_5PPh_2W(CO)_5$ at 1643.8
Calculated	shows the height of the lines in mm of the calculated isotope pattern of $Os_3(CO)_{11}PPh_2(CH_2)_5PPh_2W(CO)_5$ generated using the Sheffield Chemputer Website

Phosphorus-phosphorus coupling is observed in $Os_3(CO)_{11}PPh_2CH_2PPh_2W(CO)_5$ and $Os_3(CO)_{11}PPh_2(CH_2)_2PPh_2W(CO)_5$ but not in the longer carbon chain molecules (n = 3 - 6) as is expected. The chemical shift values do not vary significantly with the carbon chain length.

The compounds $Os_3(CO)_{11}PPh_2CH_2PPh_2W(CO)_5$ (n = 2, 4, 5) were analyzed by elemental analysis. The results of elemental analysis are tabulated below in Table 3.8.

Table 3.8. Elemental Analysis Data of $Os_3(CO)_{11}PPh_2(CH_2)_nPPh_2W(CO)_5$

Compound	n Value	Elemental Analysis			
		Calculated		Observed	
		% C	% H	% C	% H
$Os_3(CO)_{11}PPh_2(CH_2)_nPPh_2M(CO)_5$ (M=W)	2	31.51	1.51	31.88	1.63
	4	32.44	1.73	32.6	1.81
	5	32.89	1.84	33.22	2.17

The observed % carbon and % hydrogen agree within reasonable error to the calculated values for the empirical formula of the compounds $Os_3(CO)_{11}PPh_2(CH_2)_nPPh_2W(CO)_5$ (n = 2, 4, 5).

3.2.3.2. Structural Determination of $Os_3(CO)_{11}PPh_2(CH_2)_2PPh_2W(CO)_5$

The structure of compound $Os_3(CO)_{11}PPh_2(CH_2)_2PPh_2W(CO)_5$ was determined by X-ray crystallography. A view of the molecule is shown in Figure 3.2. Some bond length and angle data are given in Table 3.9.

The X-ray crystal structure was determined in order to conclusively ascertain the structure of $Os_3(CO)_{11}PPh_2(CH_2)_2PPh_2W(CO)_5$ suggested by its infrared, mass spectroscopy, $^{31}P\{^1H\}$ NMR, and elemental analysis data.

Figure 3.2. Crystal Structure of $Os_3(CO)_{11}PPh_2(CH_2)_2PPh_2W(CO)_5$

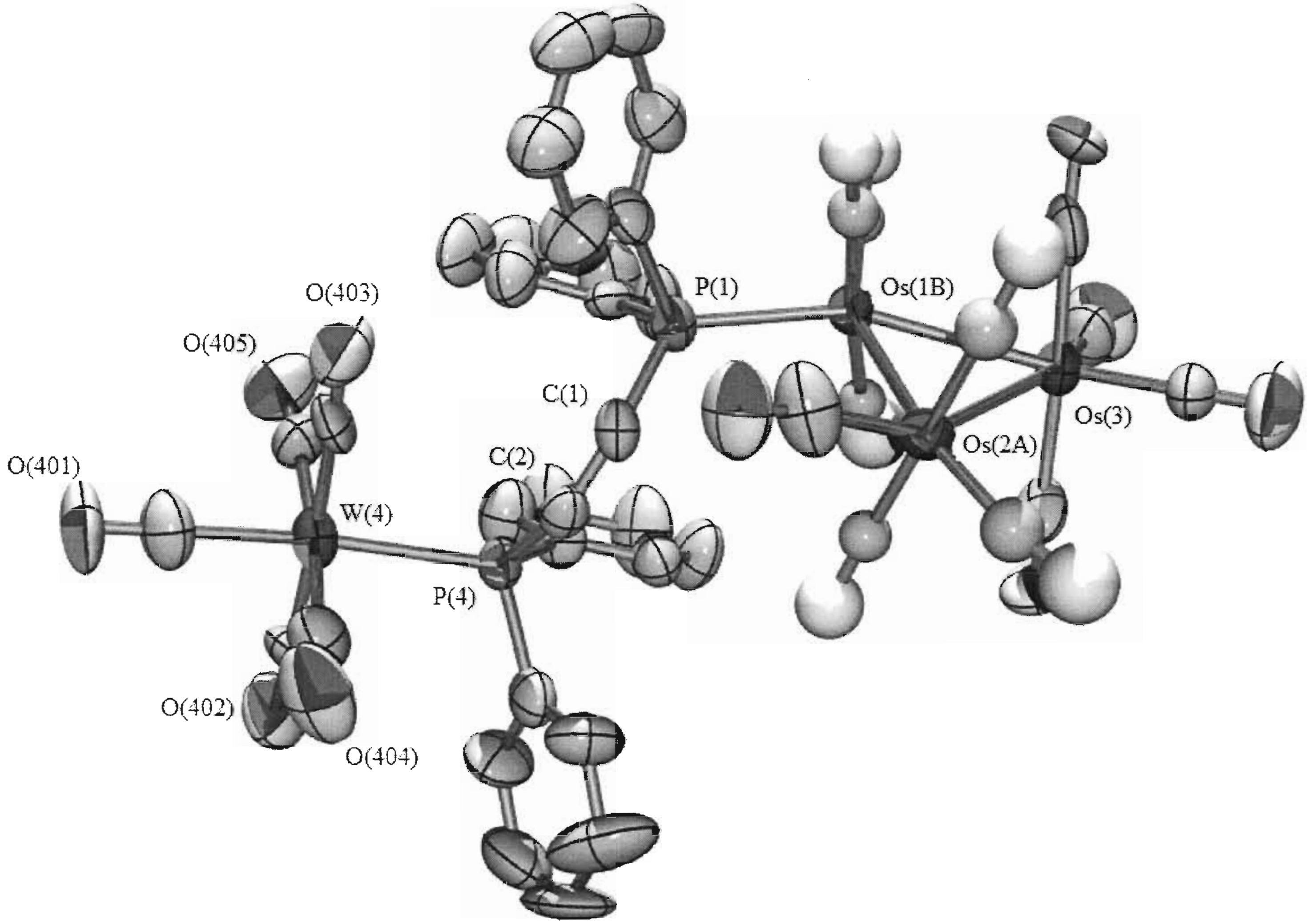

Table 3.9. Selected Bond Lengths and Angles of $Os_3(CO)_{11}PPh_2(CH_2)_2PPh_2W(CO)_5$

Bond Lengths (Å)

Os(1B)-C(13B)	1.84(2)	Os(3)-C(302)	1.89(3)
Os(1B)-(11B)	1.85(2)	Os(3)-C(303)	1.96(3)
Os(1B)-C(12B)	1.86(2)	P(1)-C(1)	1.80(2)
Os(1B)-P(1)	2.373(5)	W(4)-C(401)	1.99(2)
Os(1B)-Os(3)	2.876(2)	W(4)-C(403)	2.00(2)
Os(1B)-Os(2A)	2.911(3)	W(4)-C(404)	2.01(3)
C(11B)-O(11B)	1.25(2)	W(4)-C(402)	2.01(2)
C(12B)-O(12B)	1.22(2)	W(4)-C(405)	2.01(2)
C(13B)-O(13B)	1.20(2)	W(4)-P(4)	2.541(5)
Os(2A)-C(21A)	1.84(2)	P(4)-C(2)	1.785(19)
Os(2A)-C(22A)	1.86(2)	C(1)-C(2)	1.35(3)
Os(2A)-C(23A)	1.88(2)	C(301)-O(301)	1.13(2)
Os(2A)-C(24A)	1.96(3)	C(302)-O(302)	1.20(3)
Os(2A)-Os(3)	2.8857(19)	C(303)-O(303)	1.11(2)
C(21A)-O(21A)	1.21(2)	C(304)-O(304)	1.15(3)
C(22A)-O(22A)	1.21(2)	C(401)-O(401)	1.15(3)
C(23A)-O(23A)	1.23(5)	C(402)-O(402)	1.16(3)
C(24A)-O(24A)	1.12(3)	C(403)-O(403)	1.17(2)
Os(3)-C(304)	1.87(3)	C(404)-O(404)	1.16(3)
Os(3)-C(301)	1.89(2)	C(405)-O(405)	1.15(3)

Bond Angles (deg)

C(13B)-Os(1B)-C(11B)	94(2)	C(301)-Os(3)-C(302)	90.5(9)
C(13B)-Os(1B)-C(12B)	95.2(17)	C(304)-Os(3)-C(303)	93.0(10)
C(11B)-Os(1B)-C(12B)	170.1(19)	C(301)-Os(3)-C(303)	91.2(9)
C(13B)-Os(1B)-P(1)	97.2(12)	C(302)-Os(3)-C(303)	174.1(9)
C(11B)-Os(1B)-P(1)	89.2(15)	C(304)-Os(3)-Os(1B)	97.5(7)
C(12B)-Os(1B)-P(1)	93.5(11)	C(301)-Os(3)-Os(1B)	160.5(7)
C(13B)-Os(1B)-Os(3)	98.5(12)	C(302)-Os(3)-Os(1B)	78.5(6)
C(11B)-Os(1B)-Os(3)	77.6(15)	C(303)-Os(3)-Os(1B)	98.2(6)
C(12B)-Os(1B)-Os(3)	97.1(11)	C(304)-Os(3)-Os(2A)	154.4(8)

P(1)-Os(1B)-Os(3)	160.09(16)	C(301)-Os(3)-Os(2A)	105.1(8)
C(13B)-Os(1B)-Os(2A)	155.9(12)	C(302)-Os(3)-Os(2A)	95.8(7)
C(11B)-Os(1B)-Os(2A)	91.4(15)	C(303)-Os(3)-Os(2A)	78.3(6)
C(12B)-Os(1B)-Os(2A)	78.7(12)	Os(1B)-Os(3)-Os(2A)	60.70(6)
P(1)-Os(1B)-Os(2A)	106.32(15)	C(31)-P(1)-Os(1B)	119.8(5)
Os(3)-Os(1B)-Os(2A)	59.81(6)	C(401)-W(4)-C(403)	89.7(10)
C(21A)-Os(2A)-C(22A)	92(2)	C(401)-W(4)-C(404)	87.6(10)
C(21A)-Os(2A)-C(23A)	88(2)	C(403)-W(4)-C(404)	90.2(10)
C(22A)-Os(2A)-C(23A)	178.4(19)	C(401)-W(4)-C(402)	88.0(10)
C(21A)-Os(2A)-C(24A)	105.2(17)	C(403)-W(4)-C(402)	177.6(8)
C(22A)-Os(2A)-C(24A)	98.2(14)	C(404)-W(4)-C(402)	90.1(10)
C(23A)-Os(2A)-C(24A)	80.2(17)	C(401)-W(4)-C(405)	87.3(10)
C(21A)-Os(2A)-Os(1B)	157.2(15)	C(403)-W(4)-C(405)	89.3(9)
C(22A)-Os(2A)-Os(1B)	81.4(12)	C(404)-W(4)-C(405)	174.9(9)
C(23A)-Os(2A)-Os(1B)	99.2(15)	C(402)-W(4)-C(405)	90.2(9)
C(24A)-Os(2A)-Os(1B)	97.4(8)	C(401)-W(4)-P(4)	174.3(8)
C(21A)-Os(2A)-Os(3)	99.6(15)	C(403)-W(4)-P(4)	92.4(6)
C(22A)-Os(2A)-Os(3)	94.7(12)	C(404)-W(4)-P(4)	87.0(7)
C(23A)-Os(2A)-Os(3)	86.8(15)	C(402)-W(4)-P(4)	90.0(6)
C(24A)-Os(2A)-Os(3)	151.4(9)	C(405)-W(4)-P(4)	98.1(6)
Os(3)-Os(2A)-Os(1B)	59.49(6)	C(2)-P(4)-W(4)	108.8(6)
C(304)-Os(3)-C(301)	99.0(11)	C(2)-C(1)-P(1)	139.7(16)
C(304)-Os(3)-C(302)	92.3(11)	C(1)-C(2)-P(4)	141.1(15)

The crystal structure shows the diphosphine ligand $PPh_2(CH_2)_2PPh_2$ acting as a bridge in which one phosphine is coordinated in an equatorial position to an osmium atom of the triosmium cluster, and the other phosphine is coordinated to the tungsten centre of the $W(CO)_5$ unit.

The axial carbonyls of compound $Os_3(CO)_{11}PPh_2(CH_2)_2PPh_2W(CO)_5$ show a similar staggered conformation as seen in compounds $Os_3(CO)_{11}PPh_2(CH_2)_2PPh_2$ and $Os_3(CO)_{11}PPh_2(CH_2)_2PPh_2Os_3(CO)_{11}$. The axial carbonyl C12B is tilted away from Os3 towards Os2A, while its *trans* axial carbonyl is tilted towards Os3 and slightly away from

Os2A. On Os2A, the axial carbonyls are leaning at a similar angle, with C23A leaning away from Os1B towards Os3 and C22A leaning towards Os1B away from Os3. The axial carbonyls on Os3, however are leaning the opposite direction from those of Os1B and Os2A. The axial carbonyl C303 is tilted towards Os2A away from Os1B, while C302 is leaning away from Os2A towards Os1B. The *trans* axial carbonyls are bent, showing bond angles of between 170 and 178° as was seen in compound $Os_3(CO)_{11}PPh_2(CH_2)_2PPh_2$.

As was seen in the structure of compound $Os_3(CO)_{11}PPh_2(CH_2)_2PPh_2Os_3(CO)_{11}$ the equatorial carbonyl C13B and its neighbouring phosphine P1 are twisted slightly out of the plane of the three osmium atoms. The carbonyl C13B is raised slightly above the triosmium ring, while P1 is pushed down from the plane, with respect to the view of the molecule shown in Figure 3.2.

The interatomic distances between the atoms of the osmium cluster in $Os_3(CO)_{11}PPh_2(CH_2)_2PPh_2W(CO)_5$ are not significantly different from those of the uncoordinated compound $Os_3(CO)_{11}PPh_2(CH_2)_2PPh_2$. The longest bond distances are those of the Os-Os bonds, at an average of 2.89 Å.

3.3. Discussion

$Os_3(CO)_{11}PPh_2(CH_2)_nPPh_2M(CO)_5$ (M=W, Cr, Mo) (n=1-6)

Compounds $Os_3(CO)_{11}PPh_2(CH_2)_nPPh_2Cr(CO)_5$, $Os_3(CO)_{11}PPh_2(CH_2)_nPPh_2Mo(CO)_5$, and $Os_3(CO)_{11}PPh_2(CH_2)_nPPh_2W(CO)_5$ were prepared by freezing $Os_3(CO)_{11}PPh_2(CH_2)_nPPh_2$ dissolved in dichloromethane to liquid nitrogen temperature and then adding a layer of $M(CO)_5THF$ dissolved in THF. The second layer was frozen to liquid nitrogen temperature and the vessel containing the two frozen layers was put in the freezer, allowing the two frozen layers to slowly melt together to form the compounds in a very high yield (~95%).

Scheme 3.1. Preparation of $Os_3(CO)_{11}PPh_2(CH_2)_nPPh_2M(CO)_5$

$$Os_3(CO)_{11}PPh_2(CH_2)_nPPh_2 + M(CO)_5THF \longrightarrow Os_3(CO)_{11}PPh_2(CH_2)_nPPh_2M(CO)_5$$

(M=W, Cr, Mo) (n = 1 - 6)

Although $Os_3(CO)_{11}PPh_2CH_2PPh_2Os_3(CO)_{11}$ could not be prepared, the $M(CO)_5$ unit seems to be less sterically demanding than the $Os_3(CO)_{11}$ unit since this compound $Os_3(CO)_{11}PPh_2CH_2PPh_2M(CO)_5$ was prepared in nearly 95% yield.

A few trends were observed with respect to the crystallization of these compounds. Compounds $Os_3(CO)_{11}PPh_2(CH_2)_nPPh_2Cr(CO)_5$, $Os_3(CO)_{11}PPh_2(CH_2)_nPPh_2Mo(CO)_5$, and $Os_3(CO)_{11}PPh_2(CH_2)_nPPh_2W(CO)_5$ with n = 1, 2, 4, and 5 formed crystals readily, however the n = 3 and 6 analogues could not be obtained in crystalline form. Also, the $Os_3(CO)_{11}PPh_2(CH_2)_nPPh_2Cr(CO)_5$ and $Os_3(CO)_{11}PPh_2(CH_2)_nPPh_2W(CO)_5$ compounds crystallized more readily than the $Os_3(CO)_{11}PPh_2(CH_2)_nPPh_2Mo(CO)_5$ compounds, which were more disposed to decomposition than crystallization.

In terms of spectroscopy, the coordination of the dangling phosphine of $Os_3(CO)_{11}PPh_2(CH_2)_nPPh_2$ to the group 6 metal centre is not expected to have a large effect on the stretching frequency of the carbonyls of the osmium cluster since these are quite far removed from the group 6 metal centre. By comparing the IR spectrum of the uncoordinated $Os_3(CO)_{11}PPh_2(CH_2)_nPPh_2$ with that of the metal coordinated $Os_3(CO)_{11}PPh_2(CH_2)_nPPh_2Cr(CO)_5$, $Os_3(CO)_{11}PPh_2(CH_2)_nPPh_2Mo(CO)_5$, and $Os_3(CO)_{11}PPh_2(CH_2)_nPPh_2W(CO)_5$ the stretching frequencies of the carbonyls due to the $Os_3(CO)_{11}PPh_2(CH_2)_nPPh_2$ unit thus remain largely unchanged. The bands below 1955 cm^{-1} can be mainly attributed to the carbonyls on the group 6 $M(CO)_5$ unit, while the bands in the region 1956-2110 cm^{-1} are mainly due to the $Os_3(CO)_{11}PPh_2(CH_2)_nPPh_2$ unit and remain unaffected. Conversely, when comparing the IR spectrum of $M(CO)_6$ with that of the phosphine coordinated compounds $Os_3(CO)_{11}PPh_2(CH_2)_nPPh_2Cr(CO)_5$, $Os_3(CO)_{11}PPh_2(CH_2)_nPPh_2Mo(CO)_5$, and $Os_3(CO)_{11}PPh_2(CH_2)_nPPh_2W(CO)_5$ the carbonyl bands are shifted to significantly lower frequencies. For example, in $W(CO)_6$ the carbonyl band occurs at 1983 cm^{-1} while in compound $Os_3(CO)_{11}PPh_2(CH_2)_2PPh_2W(CO)_5$, the carbonyl bands due to the $W(CO)_5$ unit occur at 1951(m) and 1941(s) cm^{-1}.

This decrease in vibrational energy reflects the increase in electron density at the tungsten centre from the σ-donating phosphine, thus increasing the backbonding to the carbonyls bound to tungsten.

An $M(CO)_5L$ unit is expected to have three infrared active carbonyl bands: two a_1 bands plus one e band.[25] This is indeed observed: two bands are observed for the $W(CO)_5L$ unit, with a small shoulder above the 1951 cm^{-1} band. The a_1 band occurs at 1941(s) cm^{-1} and the e band at 1951(m) cm^{-1}. The small shoulder corresponds to the second a_1 mode, which arises due to stretching of the CO *trans* to the phosphine ligand, and is often observed as a weak shoulder.[25]

The $^{31}P\{^1H\}$ NMR of the compounds $Os_3(CO)_{11}PPh_2(CH_2)_nPPh_2Cr(CO)_5$, $Os_3(CO)_{11}PPh_2(CH_2)_nPPh_2Mo(CO)_5$, and $Os_3(CO)_{11}PPh_2(CH_2)_nPPh_2W(CO)_5$ show two phosphorus signals: one due to the phosphine bound to the osmium cluster and one due to the phosphine bound to the group 6 metal. As was observed in compound $Os_3(CO)_{11}PPh_2(CH_2)_nPPh_2$, the two phosphorus atoms couple to each other to give two doublets only with n values of two or less. Although the chemical shift of the phosphine bound to the osmium cluster remains relatively unchanged, the spectrum shows a decrease in chemical shift of the phosphine bound to the group 6 metal as we move down the group. This reflects the increase in shielding as we move down the group.

3.4. Conclusion

The synthesis and characterization of a series of the bidentate phosphine bridged compounds $Os_3(CO)_{11}PPh_2(CH_2)_nPPh_2M(CO)_5$ for M = Cr, Mo, and W (n = 1 - 6) have been presented. The compounds have been characterized by infrared, $^{31}P\{^1H\}$ NMR and mass spectroscopy, and X-ray crystallography.

3.5. Experimental

3.5.1. General Methods

Unless otherwise stated, all starting materials and products in this chapter were handled under an inert atmosphere of nitrogen using standard Schlenk techniques. The masses and volumes listed in the preparation of compounds are approximate.

3.5.2. Materials

Hexanes was refluxed over potassium, distilled and stored under nitrogen. THF was treated the same but benzophenone was added as an indicator of dryness.

Acetonitrile and dichloromethane were refluxed over CaH_2, distilled and stored under nitrogen. $PPh_2(CH_2)_nPPh_2$ (n = 1 - 4) were obtained commercially from Strem Chemicals Inc. and $PPh_2(CH_2)_nPPh_2$ (n = 5, 6) from Aldrich Chemicals Company. OsO_4 was obtained commercially from Pressure Chemical Company and $Os_3(CO)_{12}$ was prepared by a literature method. $Cr(CO)_6$, $Mo(CO)_6$, and $W(CO)_6$ were obtained commercially from Strem Chemicals Inc. $Cr(CO)_5(THF)$, $Mo(CO)_5(THF)$, and $W(CO)_5(THF)$ were prepared by literature methods.[26]

3.5.3. Instrumentation

Infrared Spectra were recorded on a Bomem MB-Series spectrophotometer; samples were contained in cells with NaCl windows. $^{31}P\{^1H\}$ NMR were recorded by Mr. Colin Zhang at Simon Fraser University on either a Brucker Avance 600 NMR instrument at an operating frequency of 242.925 MHz or a Varian Mercury 400 NMR instrument at an operating frequency of 161.965 MHz. Elemental analyses were performed by M. K. Yang at the Microanalytical Laboratory at Simon Fraser University. Mass Spectroscopy (LSIMS) was performed by David McGillivray at the University of Victoria. X-ray crystallography was performed by Dr. Michael Jennings at the University of Western Ontario.

3.5.4. Preparation of Compounds

Preparation of $Os_3(CO)_{11}PPh_2(CH_2)_2PPh_2W(CO)_5$

To a schlenk tube was added a solution of excess $W(CO)_5THF$ (23 mg, 0.06 mmol) in THF (10 mL). The tube was cooled to −196 °C and with continued cooling was added a solution of $Os_3(CO)_{11}PPh_2(CH_2)_2PPh_2$ (50 mg, 0.039 mmol) in dichloromethane (5 mL). The tube was stored in the freezer for 1 to 6 days and then the solution was evaporated to dryness and the solid subjected to column chromatography on a silica gel column. Elution with hexane / CH_2Cl_2 (80 / 20 by volume) gave a yellow band of the desired compound (yield ~ 95 %). $Os_3(CO)_{11}PPh_2(CH_2)_2PPh_2W(CO)_5$ was recrystallized from hexane / CH_2Cl_2 to give orange crystals. All other compounds presented in this chapter were prepared in a similar manner. $Os_3(CO)_{11}PPh_2CH_2PPh_2Cr(CO)_5$: IR hexanes υ(CO) 2108 (w), 2064 (m), 2056 (m), 2035 (m), 2020 (s), 2004 (w), 1991 (m), 1978 (w,b), 1954 (m), 1939 (s) cm^{-1}; MS (LSIMS) *m/z* 1452.6 (Calcd = 1456 (100%)); $^{31}P\{^1H\}$ NMR ($CDCl_3$) δ –7.5 (d), 57.6 (d) ppm. $Os_3(CO)_{11}PPh_2(CH_2)_2PPh_2Cr(CO)_5$: IR hexanes υ(CO) 2108 (m), 2064 (m), 2056 (s), 2034 (m), 2020 (s), 2003 (w), 1991 (m), 1983 (w,b), 1954 (m), 1939 (s) cm^{-1}; MS (LSIMS) *m/z* 1467.5 (Calcd = 1470 (100%)); $^{31}P\{^1H\}$ NMR ($CDCl_3$) δ –7.8 (d), 50.6 (d) ppm. Elemental Analysis Calculated for $Os_3CrP_2C_{42}O_{16}H_{24}$: 34.33 %C; 1.65 %H. Observed: 34.17 %C; 1.61 %H. $Os_3(CO)_{11}PPh_2(CH_2)_3PPh_2Cr(CO)_5$: IR hexanes υ(CO) 2107 (w), 2064 (w), 2055 (m), 2035 (m), 2019 (s), 2002 (w), 1991 (m), 1982 (w), 1966 (w), 1951 (m), 1941 (s) cm^{-1}; MS (LSIMS) *m/z* 1483.6 (Calcd = 1484 (100%)); $^{31}P\{^1H\}$ NMR ($CDCl_3$) δ –8.8 (s), 47.7 (s) ppm. $Os_3(CO)_{11}PPh_2(CH_2)_4PPh_2Cr(CO)_5$: IR hexanes υ(CO) 2108 (w), 2063 (m), 2055 (m), 2035 (m), 2020 (s), 2002 (w), 1991 (m), 1982 (w,b), 1951 (m), 1939 (s) cm^{-1}; MS (LSIMS) *m/z* 1497.6 (Calcd = 1498 (100%)); $^{31}P\{^1H\}$ NMR ($CDCl_3$) δ –9.0 (s), 46.4 (s) ppm; Elemental Analysis Calculated for $Os_3CrP_2C_{44}O_{16}H_{28}$: 35.29 %C; 1.88 %H. Observed: 35.55 %C; 1.96 %H. $Os_3(CO)_{11}PPh_2(CH_2)_5PPh_2Cr(CO)_5$: IR hexanes υ(CO) 2107 (w), 2063 (m), 2055 (m), 2035 (m), 2020 (s), 2002 (w), 1990 (m), 1982 (w,b), 1950 (m), 1938 (s) cm^{-1}; MS (LSIMS) *m/z* 1511.9 (Calcd = 1512 (100%)); $^{31}P\{^1H\}$ NMR ($CDCl_3$) δ –7.1 (s), 47.2 (s) ppm; Elemental Analysis Calculated for $Os_3CrP_2C_{45}O_{16}H_{30}$:

35.76 %C; 2.00 %H. Observed: 35.55 %C; 2.11 %H. $Os_3(CO)_{11}PPh_2(CH_2)_6PPh_2Cr(CO)_5$: IR hexanes υ(CO) 2107 (m), 2063 (m), 2055 (m), 2034 (m), 2019 (s), 2002 (w), 1990 (m), 1981 (w,b), 1949 (m), 1938 (s) cm^{-1}; MS (LSIMS) *m/z* 1525.8 (Calcd = 1526 (100%)); ^{31}P NMR ($CDCl_3$) δ –8.8 (s), 46.2 (s) ppm. $Os_3(CO)_{11}PPh_2CH_2PPh_2Mo(CO)_5$: IR hexanes υ(CO) 2108 (m), 2072 (m), 2056 (m), 2035 (m), 2020 (s), 2004 (w), 1991 (m), 1980 (w,b), 1951 (s), 1937 (s) cm^{-1}; MS (LSIMS) *m/z* 1497.5 (Calcd = 1500 (100%)). $Os_3(CO)_{11}PPh_2(CH_2)_2PPh_2Mo(CO)_5$: IR hexanes υ(CO) 2108 (w), 2073 (m), 2056 (m), 2034 (m), 2021 (s), 2003 (w), 1992 (m), 1980 (w,b), 1952 (m), 1939 (s) cm^{-1}; MS (LSIMS) *m/z* 1511.7 (Calcd = 1514 (100%)); $^{31}P\{^1H\}$ NMR ($CDCl_3$) δ –7.8 (d), 31.2 (d) ppm; Elemental Analysis Calculated for $Os_3MoP_2C_{42}O_{16}H_{24}$: 33.34 %C; 1.60 %H. Observed: 33.55 %C; 1.79 %H. $Os_3(CO)_{11}PPh_2(CH_2)_3PPh_2Mo(CO)_5$: IR hexanes υ(CO) 2107 (w), 2072 (m), 2055 (m), 2035 (m), 2020 (s), 2002 (w), 1991 (m), 1980 (w), 1967 (w), 1949 (s), 1940 (s) cm^{-1}; MS (LSIMS) *m/z* 1525.5 (Calcd = 1528 (100%)); $^{31}P\{^1H\}$ NMR ($CDCl_3$) δ –9.6 (s), 27.8 (s) ppm. $Os_3(CO)_{11}PPh_2(CH_2)_4PPh_2Mo(CO)_5$: IR hexanes υ(CO) 2108 (w), 2072 (m), 2055 (m), 2035 (m), 2020 (s), 2002 (w), 1991 (m), 1981 (w,b), 1949 (m), 1938 (s) cm^{-1}; MS (LSIMS) *m/z* 1540.6 (Calcd = 1542 (100%)); $^{31}P\{^1H\}$ NMR ($CDCl_3$) δ –8.8 (s), 27.9 (s) ppm. $Os_3(CO)_{11}PPh_2(CH_2)_5PPh_2Mo(CO)_5$: IR hexanes υ(CO) 2107 (w), 2071 (m), 2055 (m), 2034 (m), 2019 (s), 2002 (w), 1991 (m), 1980 (w,b), 1948 (m), 1937 (s) cm^{-1}; MS (LSIMS) *m/z* 1556.6 (Calcd = 1556 (100%)); $^{31}P\{^1H\}$ NMR ($CDCl_3$) δ –7.1 (s), 28.8 (s) ppm. $Os_3(CO)_{11}PPh_2(CH_2)_6PPh_2Mo(CO)_5$: IR hexanes υ(CO) 2107 (w), 2071 (m), 2055 (m), 2035 (m), 2020 (s), 2002 (w), 1991 (m), 1980 (w,b), 1948 (m), 1937 (s) cm^{-1}; MS (LSIMS) *m/z* 1569.7 (Calcd = 1570 (100%)); $^{31}P\{^1H\}$ NMR ($CDCl_3$) δ –8.6 (s), 27.9 (s) ppm. $Os_3(CO)_{11}PPh_2CH_2PPh_2W(CO)_5$: IR hexanes υ(CO) 2107 (m), 2072 (m), 2056 (s), 2035 (m), 2020 (s), 2004 (w), 1991 (m), 1980 (w,b), 1951 (s), 1937 (s) cm^{-1}; MS (LSIMS) *m/z* 1586.5 (Calcd = 1588 (100%)); $^{31}P\{^1H\}$ NMR ($CDCl_3$) δ –7.9 (d), 14.8 (d) ppm. $Os_3(CO)_{11}PPh_2(CH_2)_2PPh_2W(CO)_5$: IR hexanes υ(CO) 2108 (w), 2073 (w), 2056 (m), 2034 (m), 2021 (s), 2003 (w), 1992 (m), 1980 (w,b), 1952 (m), 1939 (s) cm^{-1}; MS (LSIMS) *m/z* 1599.7 (Calcd = 1602 (100%)); $^{31}P\{^1H\}$ NMR ($CDCl_3$) δ –8.2 (d), 12.2 (d) ppm; Elemental Analysis Calculated for $Os_3WP_2C_{42}O_{16}H_{24}$: 31.51 %C; 1.51 %H. Observed: 31.88 %C; 1.63 %H. $Os_3(CO)_{11}PPh_2(CH_2)_3PPh_2W(CO)_5$: IR hexanes υ(CO) 2107 (w), 2072 (m), 2055 (m), 2035 (m), 2020 (s), 2002 (w), 1991 (m), 1980 (w), 1966 (w), 1949 (s), 1940 (s) cm^{-1}; MS (LSIMS) *m/z* 1615.6 (Calcd = 1616 (100%)); $^{31}P\{^1H\}$ NMR ($CDCl_3$) δ –8.7 (s), 10.2 (s) ppm. $Os_3(CO)_{11}PPh_2(CH_2)_4PPh_2W(CO)_5$: IR hexanes υ(CO) 2108 (w), 2072 (m), 2055 (m), 2035 (m), 2020 (s), 2002 (w), 1991 (m), 1981 (w,b), 1949 (s), 1938 (s) cm^{-1}; MS (LSIMS) *m/z* 1629.6 (Calcd = 1630 (100%)); $^{31}P\{^1H\}$ NMR ($CDCl_3$) δ –8.9 (s), 9.5 (s) ppm; Elemental Analysis Calculated for $Os_3WP_2C_{44}O_{16}H_{28}$: 32.44 %C; 1.73 %H. Observed: 32.60 %C; 1.81 %H. $Os_3(CO)_{11}PPh_2(CH_2)_5PPh_2W(CO)_5$: IR hexanes υ(CO) 2107 (w), 2071 (w), 2055 (m), 2034 (m), 2019 (s), 2002 (w), 1990 (m), 1980 (w,b), 1948 (m), 1937 (s) cm^{-1}; MS (LSIMS) *m/z* 1643.8 (Calcd = 1644 (100%)); $^{31}P\{^1H\}$ NMR ($CDCl_3$) δ –8.3 (s), 9.8 (s) ppm; Elemental Analysis Calculated for $Os_3WP_2C_{45}O_{16}H_{30}$: 32.89 %C; 1.84 %H. Observed: 33.22 %C; 2.17 %H. $Os_3(CO)_{11}PPh_2(CH_2)_6PPh_2W(CO)_5$: IR hexanes υ(CO) 2107 (w), 2071 (w), 2055 (m), 2035 (m), 2020 (s), 2002 (w), 1990 (m), 1980 (w,b), 1948 (s), 1937 (s) cm^{-1}; MS (LSIMS) *m/z* 1657.8 (Calcd = 1658 (100%)); $^{31}P\{^1H\}$ NMR ($CDCl_3$) δ –8.6 (s), 9.8 (s) ppm.

CHAPTER 4

THE RHENIUM DERIVATIVES OF $Os_3(CO)_{11}PPh_2(CH_2)_nPPh_2$

4.1. Introduction

In the present chapter is presented the synthesis and characterization of the bidentate phosphine bridged compounds $Os_3(CO)_{11}PPh_2(CH_2)_nPPh_2Re(CO)_4Br$ and $[Os_3(CO)_{11}PPh_2(CH_2)_nPPh_2]_2Re(CO)_3Br$. These compounds of the type $[ReBr(CO)_4L]$ and $[ReBr(CO)_3L_2]$, where L is the ligand $Os_3(CO)_{11}PPh_2(CH_2)_nPPh_2$ (n = 2, 4), form an extension of the study of the substitution reactions of $Re(CO)_5Br$, which is well documented in the literature.[27]

In 1965 the group of Jolly and Stone[28] prepared a mixture of the *cis and trans* isomers of $[Re(CO)_4Br(PPh_3)]$. They irradiated triphenylphosphine and decacarbonyldirhenium in cyclohexane to form the dimer $[Re(CO)_4(PPh_3)]_2$, then treated it with bromine in carbon tetrachloride at 0 °C. They found that, although the *trans* isomer is stable at room temperature, it could be completely isomerized to form the *cis* isomer in refluxing chloroform. Furthermore, they found that a purely *cis* product could be prepared by refluxing $Re(CO)_5Br$ and triphenylphosphine in chloroform.

In 2003 the group of Beckett *et al.*[27] prepared a series of compounds of the type $[MBr(CO)_3L_2]$ where M = Mn or Re and L was various triorganophosphines including $P(C_6H_4Cl\text{-}4)_3$, $P(C_6H_4OMe\text{-}4)_3$, $P(CH_2C_6H_4)_3$, $PPh_2(CH_2)_2PPh_2$, $PPh_2(CH_2)_3PPh_2$, and $PPh_2(CH_2)_4PPh_2$. These were prepared as precursors for some metallatetraborane derivatives. They found that although the geometrical configuration about the metal centre (Mn or Re) could be *mer cis-, mer trans-, or fac cis-* the rhenium compounds favored exclusively the *fac cis-* arrangement, while the manganese compounds tended to be either *fac cis-* or *mer trans-*. The *mer cis-* configuration was unknown. This was evidenced by IR spectra, ^{31}P NMR spectra, and several crystal structures.

In 1973 Reimann and Singleton[29] prepared a series of *fac, cis-*[ReBr(CO)$_3$L$_2$] where L was a variety of phosphines, and thermally isomerized them to form the *mer, trans-* isomer. This was effected by refluxing the *fac, cis-* isomer in high boiling solvents; for example, in the case of *fac, cis-*[ReBr(CO)$_3$(PMe$_3$)$_2$] the compound was heated in an evacuated tube for 10 hours at 150 °C to produce *mer, trans-*[ReBr(CO)$_3$(PMe$_3$)$_2$].

Reimann and Singleton[29] also studied the trisubstitution of Re(CO)$_5$Br which had already been well documented for the manganese analogue. Refluxing Re(CO)$_5$Br with an excess of the tertiary phosphine ligand L in benzene/ petroleum ether at 100-120 °C for 15 hours yielded the trisubstituted compound *mer, cis-* [Re(CO)$_2$L$_3$Br] for a variety of phosphine ligands.

The compounds [ReBr(CO)$_4$L] and [ReBr(CO)$_3$L$_2$], where L is the ligand Os$_3$(CO)$_{11}$PPh$_2$(CH$_2$)$_n$PPh$_2$ ($n = 2, 4$), form a logical progression of these studies, and as such their synthesis and characterization is presented in this chapter.

4.2. Results

4.2.1. Os$_3$(CO)$_{11}$PPh$_2$(CH$_2$)$_n$PPh$_2$Re(CO)$_4$Br

4.2.1.1. Synthesis of Os$_3$(CO)$_{11}$PPh$_2$(CH$_2$)$_n$PPh$_2$Re(CO)$_4$Br

Os$_3$(CO)$_{11}$PPh$_2$(CH$_2$)$_2$PPh$_2$Re(CO)$_4$Br was prepared by reacting excess Re(CO)$_5$Br, with Os$_3$(CO)$_{11}$PPh$_2$(CH$_2$)$_2$PPh$_2$, and dichloromethane in a pressure sealed carrius tube. The reaction was heated for six days at 45 °C then the solvent was removed and the solid purified by column chromatography. The compound

$Os_3(CO)_{11}PPh_2(CH_2)_2PPh_2Re(CO)_4Br$ was recrystallized from hexane / CH_2Cl_2 to give yellow crystals.

The compound $Os_3(CO)_{11}PPh_2(CH_2)_4PPh_2Re(CO)_4Br$ was prepared in a similar manner; however, attempts to recrystallize it were unsuccessful.

The compounds $Os_3(CO)_{11}PPh_2(CH_2)_2PPh_2Re(CO)_4Br$ and $Os_3(CO)_{11}PPh_2(CH_2)_4PPh_2Re(CO)_4Br$ were analyzed by infrared spectroscopy. The absorptions in the carbonyl region for $Os_3(CO)_{11}PPh_2(CH_2)_2PPh_2Re(CO)_4Br$ are as follows: 2107 (m), 2055 (ms), 2035 (m), 2020 (s), 2003 (ms), 1991 (m), 1980 (w), 1969 (w), 1955 (w, sh), 1948 (m) cm^{-1}.

The compound $Os_3(CO)_{11}PPh_2(CH_2)_4PPh_2Re(CO)_4Br$ shows similar absorptions and, as expected, the absorptions do not vary with the length of the carbon chain.

The compounds $Os_3(CO)_{11}PPh_2(CH_2)_2PPh_2Re(CO)_4Br$ and $Os_3(CO)_{11}PPh_2(CH_2)_4PPh_2Re(CO)_4Br$ were analyzed by mass spectroscopy. Their molecular weights are tabulated in Table 4.1 below.

Table 4.1. Mass Spectroscopy Data for $Os_3(CO)_{11}PPh_2(CH_2)_nPPh_2Re(CO)_4Br$

Compound	n Value	Molecular Weight	
		Calculated	Observed
$Os_3(CO)_{11}PPh_2(CH_2)_nPPh_2Re(CO)_4Br$	2	1656	1655.8
	4	1684	1684

The mass spectra of $Os_3(CO)_{11}PPh_2(CH_2)_2PPh_2Re(CO)_4Br$ and $Os_3(CO)_{11}PPh_2(CH_2)_4PPh_2Re(CO)_4Br$ show molecular ions consistent with their molecular formulae. The isotope patterns also agree with the calculated isotopic pattern for these compounds, as shown below for $Os_3(CO)_{11}PPh_2(CH_2)_4PPh_2Re(CO)_4Br$ in Figure 4.1.

Figure 4.1. Comparison of Observed and Calculated Isotopic Patterns of $Os_3(CO)_{11}PPh_2(CH_2)_4PPh_2Re(CO)_4Br$

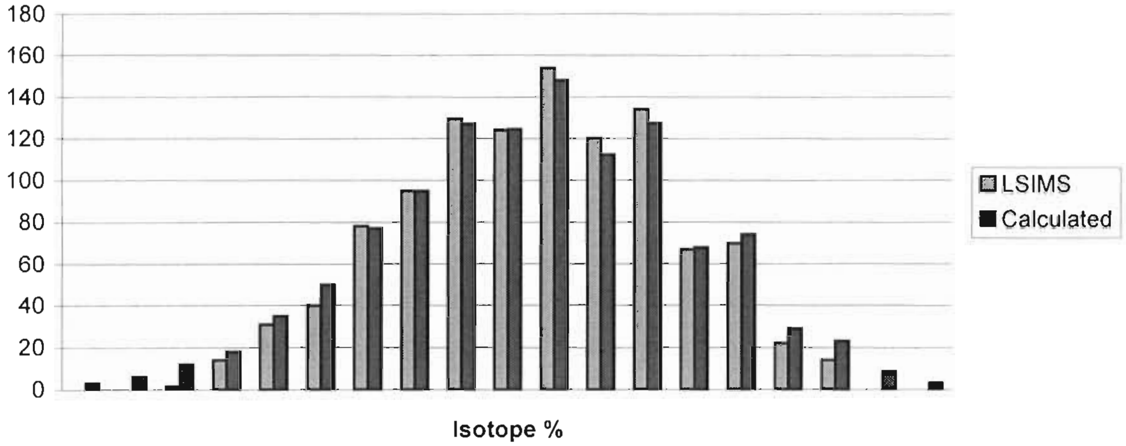

LSIMS	shows the height of the lines in mm of the molecular ion peak of $Os_3(CO)_{11}PPh_2(CH_2)_4PPh_2Re(CO)_4Br$ at 1684
Calculated	shows the height of the lines in mm of the calculated isotope pattern of $Os_3(CO)_{11}PPh_2(CH_2)_4PPh_2Re(CO)_4Br$ generated using the Sheffield Chemputer Website

The compounds $Os_3(CO)_{11}PPh_2(CH_2)_2PPh_2Re(CO)_4Br$ and $Os_3(CO)_{11}PPh_2(CH_2)_4PPh_2Re(CO)_4Br$ were analyzed $^{31}P\{^1H\}$ NMR Spectroscopy. Their chemical shifts are tabulated in Table 4.2 below.

Table 4.2. $^{31}P\{^1H\}$ NMR Resonances of $Os_3(CO)_{11}PPh_2(CH_2)_nPPh_2Re(CO)_4Br$

Compound	n Value	^{31}P NMR Resonances	
$Os_3(CO)_{11}PPh_2(CH_2)_nPPh_2Re(CO)_4Br$	2	-2.3 (d)	-7.2 (d)
	4	-3.7 (s)	-7.4 (s)

The $^{31}P\{^1H\}$ NMR spectra of $Os_3(CO)_{11}PPh_2(CH_2)_2PPh_2Re(CO)_4Br$ and $Os_3(CO)_{11}PPh_2(CH_2)_4PPh_2Re(CO)_4Br$ show two resonance signals indicating that there are two distinct phosphorus atoms in the molecules. Phosphorus-phosphorus coupling is observed in $Os_3(CO)_{11}PPh_2(CH_2)_2PPh_2Re(CO)_4Br$ but not in $Os_3(CO)_{11}PPh_2(CH_2)_4PPh_2Re(CO)_4Br$, as is expected. The chemical shift values do not vary significantly with the carbon chain length.

The compound $Os_3(CO)_{11}PPh_2(CH_2)_2PPh_2Re(CO)_4Br$ was analyzed by elemental analysis. The observed % carbon was 29.81 and % hydrogen was 1.49, in agreement with the calculated values of 29.75 % carbon and 1.46 % hydrogen for the empirical formula $Os_3ReP_2BrC_{41}O_{15}H_{24}$.

4.2.2. $[Os_3(CO)_{11}PPh_2(CH_2)_nPPh_2]_2Re(CO)_3Br$

4.2.2.1 Synthesis of $[Os_3(CO)_{11}PPh_2(CH_2)_nPPh_2]_2Re(CO)_3Br$

Preparation of the compound $[Os_3(CO)_{11}PPh_2(CH_2)_2PPh_2]_2Re(CO)_3Br$ included combining $Re(CO)_5Br$, excess $Os_3(CO)_{11}PPh_2(CH_2)_2PPh_2$ and dichloromethane in a pressure sealed carrius tube. The reaction was heated for six days at 45 °C. The solvent was removed and the solid purified by column chromatography then recrystallized from hexane / CH_2Cl_2 to give yellow crystals.

The compound $[Os_3(CO)_{11}PPh_2(CH_2)_4PPh_2]_2Re(CO)_3Br$ was prepared in a similar manner; however, attempts to recrystallize it were unsuccessful.

The compounds $[Os_3(CO)_{11}PPh_2(CH_2)_2PPh_2]_2Re(CO)_3Br$ and $[Os_3(CO)_{11}PPh_2(CH_2)_4PPh_2]_2Re(CO)_3Br$ were analyzed by infrared spectroscopy. The absorptions in the carbonyl region for $[Os_3(CO)_{11}PPh_2(CH_2)_2PPh_2]_2Re(CO)_3Br$ are as follows: 2107 (w), 2054 (m), 2046 (w), 2035 (m), 2019 (s), 2003 (w), 1990 (w), 1983 (w), 1957 (w, b), 1915 (w) cm^{-1}. The compound $[Os_3(CO)_{11}PPh_2(CH_2)_4PPh_2]_2Re(CO)_3Br$

shows similar absorptions and, as expected, the absorptions do not vary with the length of the carbon chain.

The compounds $[Os_3(CO)_{11}PPh_2(CH_2)_2PPh_2]_2Re(CO)_3Br$ and $[Os_3(CO)_{11}PPh_2(CH_2)_4PPh_2]_2Re(CO)_3Br$ were analyzed by mass spectroscopy. Their molecular weights are tabulated in Table 4.3 below.

Table 4.3. Mass Spectroscopy Data of $[Os_3(CO)_{11}PPh_2(CH_2)_nPPh_2]_2Re(CO)_3Br$

Compound	n Value	LSIMS	
		Calculated	Observed
$[Os_3(CO)_{11}PPh_2(CH_2)_nPPh_2]_2Re(CO)_3Br$	2	2905	2905
	4	2961	2959

The mass spectra of $[Os_3(CO)_{11}PPh_2(CH_2)_2PPh_2]_2Re(CO)_3Br$ and $[Os_3(CO)_{11}PPh_2(CH_2)_4PPh_2]_2Re(CO)_3Br$ show molecular ions consistent with their molecular formulae.

The compound $[Os_3(CO)_{11}PPh_2(CH_2)_2PPh_2]_2Re(CO)_3Br$ was analyzed by $^{31}P\{^1H\}$ NMR Spectroscopy. The spectrum shows two resonances, a doublet at –9.8 ppm and a doublet at –14.1 ppm, signals indicating that there are two distinct phosphorus atoms in the molecule.

4.3. Discussion

$Os_3(CO)_{11}PPh_2(CH_2)_nPPh_2Re(CO)_4Br$ (n = 2, 4)

Compound $Os_3(CO)_{11}PPh_2(CH_2)_nPPh_2Re(CO)_4Br$ was prepared by combining $Os_3(CO)_{11}PPh_2(CH_2)_nPPh_2$ and excess $Re(CO)_5Br$ in dichloromethane and degassing. The mixture was heated in a 45 °C oil bath for 6 days. Although

$[Os_3(CO)_{11}PPh_2(CH_2)_nPPh_2]_2Re(CO)_3Br$ was produced as a side product, the two compounds were easily separated by column chromatography.

Scheme 4.1. Preparation of $Os_3(CO)_{11}PPh_2(CH_2)_nPPh_2Re(CO)_4Br$

$$Os_3(CO)_{11}PPh_2(CH_2)_nPPh_2 + Re(CO)_5Br \longrightarrow Os_3(CO)_{11}PPh_2(CH_2)_nPPh_2Re(CO)_4Br$$

$$(n = 2, 4) \qquad + [Os_3(CO)_{11}PPh_2(CH_2)_nPPh_2]_2Re(CO)_3Br$$

Compound $Os_3(CO)_{11}PPh_2(CH_2)_nPPh_2Re(CO)_4Br$ is yellow and shows good stability in air for a several week period.

Assuming the $Re(CO)_4BrP$ unit is pseudo-octahedral, then two possible isomers exist, as shown in Figure 4.2.

Figure 4.2. The Two Possible Configurations of The $Re(CO)_4BrP$ Unit in $Os_3(CO)_{11}PPh_2(CH_2)_nPPh_2Re(CO)_4Br$

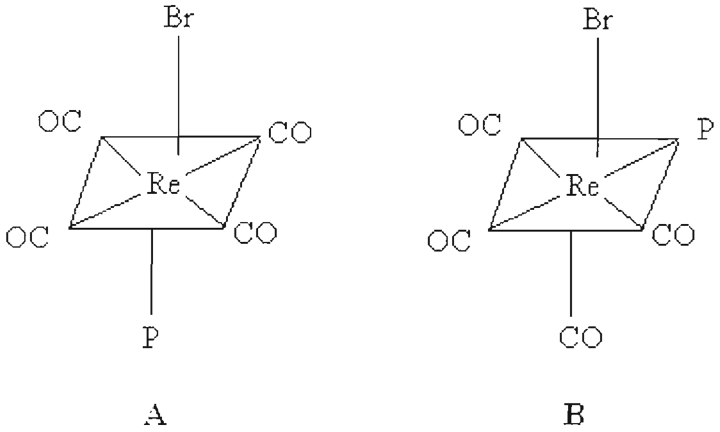

The *cis* isomer (C_s) is expected to have four infrared-active CO bands,[25] $2a_1$, b_1, and b_2. The *trans* (C_{4v}) is expected to have two infrared-active CO bands,[30] the a_1 and e_u.

The ν(CO) (hexanes) of $Os_3(CO)_{11}PPh_2(CH_2)_2PPh_2Re(CO)_4Br$ are 2107 (m), 2055 (ms), 2035 (m), 2020 (s), 2003 (ms), 1991 (m), 1980 (w), 1969 (w), 1955 (w, sh), 1948 (m) cm^{-1}. If we assume that the stretching frequencies of the carbonyls on the triosmium cluster are unaffected by the coordination of the $[Re(CO)_4Br]$ unit, since they are so far removed, then we may assign the stretches below 1955 cm^{-1} to the $Os_3(CO)_{11}PPh_2(CH_2)_nPPh_2$ unit. In this case the band at 1948 cm^{-1} and the shoulder at 1955 cm^{-1} may lead one to believe that the configuration of the $Os_3(CO)_{11}PPh_2(CH_2)_nPPh_2Re(CO)_4Br$ is *trans*. This, however, is misleading.

The published compound[28] *trans*- $[Re(CO)_4Br(PPh_3)]$ shows ν(CO) (cyclohexane) 2105 (w) and 1995 (vs) cm^{-1}. These carbonyl stretches, even accounting for the different solvents used in the spectrum, are at much higher energy than those attributed to the $[Re(CO)_4Br]$ unit of $Os_3(CO)_{11}PPh_2(CH_2)_nPPh_2Re(CO)_4Br$. The compound[28] *trans*-$[Re(CO)_4Br(PPh_3)]$, on the other hand, shows ν(CO) (cyclohexane) 2100 (s), 2015 (s), 1998 (vs), and 1940 (s) cm^{-1}. It is possible that the band at 1948 cm^{-1} in the spectrum of $Os_3(CO)_{11}PPh_2(CH_2)_nPPh_2Re(CO)$ is equivalent to the band at lowest energy of *trans*-$[Re(CO)_4Br(PPh_3)]$, while the other three bands are hidden under those of the $Os_3(CO)_{11}PPh_2(CH_2)_nPPh_2$ unit.

In 1965 the group of Jolly and Stone[28] prepared a mixture of the *cis and trans* isomers of $[Re(CO)_4Br(PPh_3)]$ by irradiating triphenylphosphine and decacarbonyldirhenium in cyclohexane to form the dimer $[Re(CO)_4(PPh_3)]_2$, followed by treatment with bromine in carbon tetrachloride at 0 °C. They found that, although the *trans* isomer is stable at room temperature, it could be completely isomerized to form the *cis* isomer in refluxing chloroform.

The synthetic method used in preparing $Os_3(CO)_{11}PPh_2(CH_2)_nPPh_2Re(CO)_4Br$ utilizes six days of refluxing in dichloromethane. It seems quite likely, therefore, that even if the *trans* isomer forms initially, it is quickly isomerized under these reaction conditions to form the purely *cis* product. Indeed, Jolly and Stone[28] also found that they could prepare *cis*-$[Re(CO)_4Br(PPh_3)]$ by refluxing $Re(CO)_5Br$ and triphenylphosphine in chloroform, a procedure very similar to that presented in this thesis for the preparation of $Os_3(CO)_{11}PPh_2(CH_2)_nPPh_2Re(CO)_4Br$.

With these precedents in mind, it is proposed that the configuration about the rhenium centre of $Os_3(CO)_{11}PPh_2(CH_2)_nPPh_2Re(CO)_4Br$ is *cis,* isomer B shown in Figure 4.2.

$[Os_3(CO)_{11}PPh_2(CH_2)_nPPh_2]_2Re(CO)_3Br$ (n = 2, 4)

The preparation of compound $[Os_3(CO)_{11}PPh_2(CH_2)_nPPh_2]_2Re(CO)_3Br$ is analogous to that of compound $Os_3(CO)_{11}PPh_2(CH_2)_nPPh_2Re(CO)_4Br$ with the exception that two equivalents of $Os_3(CO)_{11}PPh_2(CH_2)_nPPh_2$ were used for each equivalent of $Re(CO)_5Br$. In practice, the yield of compound $[Os_3(CO)_{11}PPh_2(CH_2)_nPPh_2]_2Re(CO)_3Br$ was improved by adding a large excess of $Os_3(CO)_{11}PPh_2(CH_2)_nPPh_2$, which was easily removed by column chromatography. Compound $[Os_3(CO)_{11}PPh_2(CH_2)_nPPh_2]_2Re(CO)_3Br$ was yellow and sparingly soluble in hexanes. It decomposed in solvent over a period of two weeks.

Assuming the geometry at the 6-coordinate $Re(CO)_3BrP_2$ centre is octahedral, there exists three possible configurations as shown in Figure 4.3.

Figure 4.3. The Three Possible Configurations of The $Re(CO)_3BrP_2$ Centre in $[Os_3(CO)_{11}PPh_2(CH_2)_nPPh_2]_2Re(CO)_3Br$

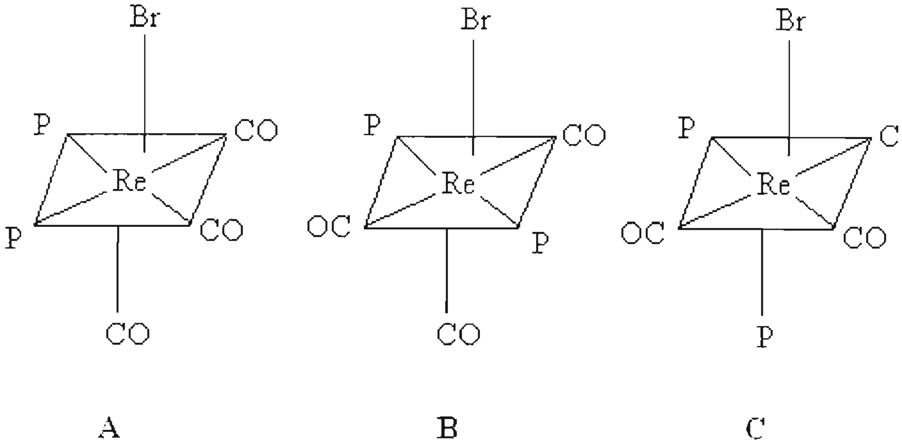

Isomer A has the two phosphines and the bromine atom in a *fac, cis-* arrangement, isomer B has a *mer, trans-* configuration with the two phosphines *trans* to each other, and isomer C has a *mer, cis-* configurations with the two phosphines *cis* to each other.

If we first consider the $^{31}P\{^1H\}$ NMR data, we observe two distinct ^{31}P resonances at chemical shifts of -9.8 and -14.2 ppm for $[Os_3(CO)_{11}PPh_2(CH_2)_2PPh_2]_2Re(CO)_3Br$. In isomer C the two phosphorus atoms on the Re centre are inequivalent, since one is *trans* and one *cis* to the bromide. In addition, the phosphorus atom coordinated to the osmium cluster is also distinct from these two. We would expect, therefore, to see at least three resonances in the $^{31}P\{^1H\}$ NMR spectrum. In isomers A and B, both of the phosphines coordinated to the Re centre are equivalent, and so we would only expect to see two resonances. On the basis of the $^{31}P\{^1H\}$ NMR data we can rule out structure C, however, we cannot distinguish between isomers A and B.

Incidently, isomer C, which has a *mer, cis-* configuration has never been prepared regardless of the choice of phosphine groups.[27] It has been prepared for the manganese analogue, but only by electrochemical means.[31]

Both isomer A (C_s) and isomer B (C_{2v}) are expected to have three infrared active bands in the carbonyl region[21]; isomer A shows $2A'+A''$ and isomer B shows $2A_1 + B_2$ bands The relative intensities of these three bands can be used to diagnose the configuration about the Re centre. The *fac, cis-* configuration (isomer A) shows three bands of approximately equal intensity, while the *mer, trans-* configuration (isomer B) shows two intense bands plus one weaker band. For example the known compound *fac, cis-* $[Re(CO)_3Br(PMe_3)_2]$ shows υ(CO) 2033 (s), 1952 (s), and 1898 (s) cm^{-1}, while *mer, trans-* $[Re(CO)_3Br(PMe_3)_2]$, prepared by thermal isomerization of *fac, cis-* $[Re(CO)_3Br(PMe_3)_2]$, shows υ(CO) 2035 (w), 1949 (s), and 1893 (m) cm^{-1}.[29]

Because the two carbonyl bands on the rhenium centre at highest energy are overlapped with the carbonyl bands due to the $Os_3(CO)_{11}PPh_2(CH_2)_nPPh_2$ fragment, we cannot compare the relative intensities of the carbonyl bands on the Re centre as a means of diagnosing the configuration. However, when the group of Beckett *et al.*[27] prepared a series of compounds of the type $[MBr(CO)_3L_2]$ where M = Mn or Re and L was various triorganophosphines including $P(C_6H_4Cl\text{-}4)_3$, $P(C_6H_4OMe\text{-}4)_3$, $P(CH_2C_6H_4)_3$ $PPh_2(CH_2)_2PPh_2$, $PPh_2(CH_2)_3PPh_2$, and $PPh_2(CH_2)_4PPh_2$, they found that although the manganese compounds tended to be either *fac, cis-* or *mer, trans-*, the rhenium compounds favored exclusively the *fac, cis-* arrangement. It seems quite probable, therefore, that $[Os_3(CO)_{11}PPh_2(CH_2)_nPPh_2]_2Re(CO)_3Br$ adopts the *fac, cis-* geometry as well.

One might also question whether *fac, cis*-$[Os_3(CO)_{11}PPh_2(CH_2)_nPPh_2]_2Re(CO)_3Br$ forms initially followed by isomerization to the *mer, trans*- configuration, since the reaction time is quite long (6 days) compared to that of Beckett *et al.*[27] (24 hours). I think that the possibility of isomerization is highly unlikely in this case. When Riemann and Singleton performed their experiments isomerizing *fac, cis*-$[ReBr(CO)_3L_2]$ to *mer, trans*-$[ReBr(CO)_3L_2]$, they found that it was necessary to add sodium borohydride to increase the labilization of the carbonyls, and heat the mixture to temperatures as high as 150 °C.[29] Since $[Os_3(CO)_{11}PPh_2(CH_2)_nPPh_2]_2Re(CO)_3Br$ was prepared by refluxing at only 45 °C, the temperature was far too low to promote isomerization. Indeed, isomerization of this compound seems improbable since the triosmium cluster would most likely decompose before the temperature necessary to promote isomerization could be reached.

Although compounds $[Os_3(CO)_{11}PPh_2(CH_2)_nPPh_2]_2Re(CO)_3Br$ and $Os_3(CO)_{11}PPh_2(CH_2)_nPPh_2Re(CO)_4Br$ were synthesized in good yield, there was no evidence found for the formation of $[Os_3(CO)_{11}PPh_2(CH_2)_nPPh_2]_3Re(CO)_2Br$ by this method.

In Reimann and Singleton's study of the trisubstitution of $Re(CO)_5Br$[29] they found that the reactions had a marked temperature effect, necessitating the use of high boiling solvents. It is likely the case that the reaction conditions were too mild to induce the formation of $[Os_3(CO)_{11}PPh_2(CH_2)_nPPh_2]_3Re(CO)_2Br$.

4.4. Conclusion

The compounds $[ReBr(CO)_4L]$ and $[ReBr(CO)_3L_2]$, where L is the ligand $Os_3(CO)_{11}PPh_2(CH_2)_nPPh_2$ (n = 2, 4) have been prepared. Due to the ambiguity in the spectroscopic data, arising from the overlap of the carbonyl bands of the triosmium portion with those of the rhenium centre the geometry at the rhenium centre could not be established without a doubt. Based on the analytical data and empirical observations of other similar published compounds $Os_3(CO)_{11}PPh_2(CH_2)_nPPh_2Re(CO)_4Br$ is postulated to have a *cis* conformation, while $[Os_3(CO)_{11}PPh_2(CH_2)_nPPh_2]_2Re(CO)_3Br$ is suggested to have a *fac, cis* conformation. The geometry could be confirmed by studying the compounds by X-ray crystallography, however no suitable crystals could be prepared.

4.5. Experimental

4.5.1. General Methods

Unless otherwise stated, all starting materials and products in this chapter were handled under an inert atmosphere of nitrogen using standard Schlenk techniques. The masses and volumes listed in the preparation of compounds are approximate.

4.5.2. Materials

Hexanes was refluxed over potassium, distilled and stored under nitrogen. Acetonitrile and dichloromethane were refluxed over CaH_2, distilled and stored under nitrogen. $PPh_2(CH_2)_nPPh_2$ (n = 1 - 4) were obtained commercially from Strem and $PPh_2(CH_2)_nPPh_2$ (n = 5, 6) from Aldrich Chemicals Company. OsO_4 was obtained commercially from Pressure Chemical Company and $Os_3(CO)_{12}$ was prepared by a literature method.[15] $Re_2(CO)_{10}$ was obtained commercially from Strem Chemicals and Br_2 was obtained commercially from The McArthur Chemical Company. $Re(CO)_5Br$ was prepared by a literature method.[32]

4.5.3. Instrumentation

Infrared Spectra were recorded on a Bomem MB-Series spectrophotometer; samples were contained in cells with NaCl windows. $^{31}P\{^1H\}$ NMR were recorded by

Mr. Colin Zhang at Simon Fraser University on either a Brucker Avance 600 NMR instrument at an operating frequency of 242.925 MHz or a Varian Mercury 400 NMR instrument at an operating frequency of 161.965 MHz. Elemental analyses were performed by M. K. Yang at the Microanalytical Laboratory at Simon Fraser University. Mass Spectroscopy (LSIMS) was performed by David McGillivray at the University of Victoria.

4.5.4. Preparation of Compounds

Preparation of $Os_3(CO)_{11}PPh_2(CH_2)_2PPh_2Re(CO)_4Br$

To a dry carrius tube was added excess $Re(CO)_5Br$ (64 mg, 0.16 mmol), $Os_3(CO)_{11}PPh_2(CH_2)_2PPh_2$ (100 mg, 0.08 mmol), and dichloromethane (20 mL). The tube was cooled to –196 °C and the solution degassed with three freeze-pump-thaw cycles and the vessel sealed under vacuum. The reaction was heated for six days at 45 °C. The solution was then evaporated to dryness and the solid subjected to column chromatography on a silica gel column. Elution with hexane / CH_2Cl_2 (65 / 35 by volume) gave a yellow band of compound $Os_3(CO)_{11}PPh_2(CH_2)_2PPh_2Re(CO)_4Br$ (yield ~ 30 %) followed by a faint yellow band of compound $[Os_3(CO)_{11}PPh_2(CH_2)_2PPh_2]_2Re(CO)_3Br$ (40 / 60 by volume). Compound $Os_3(CO)_{11}PPh_2(CH_2)_2PPh_2Re(CO)_4Br$ was recrystallized from hexane / CH_2Cl_2 to give yellow crystals.

The compound $Os_3(CO)_{11}PPh_2(CH_2)_4PPh_2Re(CO)_4Br$ was prepared in an analogous manner; however, attempts to recrystallize compound $Os_3(CO)_{11}PPh_2(CH_2)_4PPh_2Re(CO)_4Br$ were unsuccessful. $Os_3(CO)_{11}PPh_2(CH_2)_2PPh_2Re(CO)_4Br$: IR hexanes υ(CO) 2107 (m), 2055 (ms), 2035 (m), 2020 (s), 2003 (ms), 1991 (m), 1980 (w), 1969 (w), 1955 (w, sh), 1948 (m) cm^{-1}; MS (LSIMS) *m/z* 1655.8 (Calcd = 1656 (100%)); ^{31}P{^{1}H} NMR (CDCl$_3$) δ –2.3 (d), -7.2 (d) ppm; Elemental Analysis Calculated for $Os_3ReP_2BrC_{41}O_{15}H_{24}$: 29.75 %C; 1.46 %H. Observed: 29.81 %C; 1.49 %H. $Os_3(CO)_{11}PPh_2(CH_2)_4PPh_2Re(CO)_4Br$: IR hexanes υ(CO) 2107 (w), 2054 (m), 2046 (w), 2035 (w), 2020 (s), 2003 (m), 1990 (m,b), 1955 (w, sh), 1946 (m) cm^{-1}; MS (LSIMS) *m/z* 1684 (Calcd = 1684 (100%)); ^{31}P{^{1}H} NMR (CDCl$_3$) δ –3.7 (s), -7.4 (s) ppm.

Preparation of $[Os_3(CO)_{11}PPh_2(CH_2)_2PPh_2]_2Re(CO)_3Br$

To a dry carrius tube was added $Re(CO)_5Br$ (16 mg, 0.04 mmol), excess $Os_3(CO)_{11}PPh_2(CH_2)_nPPh_2$ (200 mg, 0.16 mmol), and dichloromethane (10 mL). The tube was cooled to –196 °C and the solution degassed with three freeze-pump-thaw cycles and the vessel sealed under vacuum. The reaction was heated for six days at 45 °C. The solution was then evaporated to dryness and the solid subjected to column chromatography on a silica gel column. Elution with hexane / CH_2Cl_2 (65 / 35 by volume) gave a faint yellow band of compound $Os_3(CO)_{11}PPh_2(CH_2)_2PPh_2Re(CO)_4Br$ followed by a yellow band of compound $[Os_3(CO)_{11}PPh_2(CH_2)_2PPh_2]_2Re(CO)_3Br$ (40 / 60 by volume) (yield ~ 20 %). Compound $[Os_3(CO)_{11}PPh_2(CH_2)_2PPh_2]_2Re(CO)_3Br$ was recrystallized from hexane / CH_2Cl_2 to give yellow crystals.

The compound $[Os_3(CO)_{11}PPh_2(CH_2)_4PPh_2]_2Re(CO)_3Br$ was prepared in a similar manner; however, attempts to recrystallize compound $[Os_3(CO)_{11}PPh_2(CH_2)_4PPh_2]_2Re(CO)_3Br$ were unsuccessful. $[Os_3(CO)_{11}PPh_2(CH_2)_2PPh_2]_2Re(CO)_3Br$: IR hexanes υ(CO) 2107 (w), 2054 (m), 2046 (w), 2035 (m), 2019 (s), 2003 (w), 1990 (w), 1983 (w), 1957 (w, b), 1915 (w) cm^{-1}; MS (LSIMS) *m/z* 2905 (Calcd = 2905 (100%)); $^{31}P\{^{1}H\}$ NMR ($CDCl_3$) δ –9.8 (d), -14.1 (d) ppm. $[Os_3(CO)_{11}PPh_2(CH_2)_4PPh_2]_2Re(CO)_3Br$: IR hexanes υ(CO) 2107 (w), 2054 (m), 2046 (w), 2035 (m), 2019 (s), 2003 (w), 1990 (w), 1983 (w), 1957 (w, b), 1915 (w) cm^{-1}; MS (LSIMS) *m/z* 2959 (Calcd = 2961 (100%)).

REFERENCES

1. Dyson, P.; McIndoe, J. *Transition Metal Carbonyl Cluster Chemistry.* Gordon and Breach Science Publishers: Amsterdam, The Netherlands, **2000**, chapter 1.
2. Frenking, G.; Frohlich, N. *Chem. Rev.* **2000**, 100, 717.
3. a) Graham, J. R.; Angelici, R. J. *Inorg. Chem.* **1967**, 6, 2082. b) Meier, M; Basolo, F; Pearson, R. G.; *Inorg. Chem.* **1969**, 8, 795.
4. a) Grant, S. M.; Manning, A. R. *Inorg. Chim. Acta.* **1978**, 31, 41. b) Clifford, A. F.; Mukererjce, A. K. *Inorg. Chem.* **1963**, 2, 151.
5. a) Candlin, J. P.; Shortland, A. C. *J. Organometallic Chem.* **1969**, 16, 289. b) Grant, S. M.; Manning, A. R. *Inorg. Chim. Acta.* **1978**, 31, 41.
6. Kaltsoyannis, N. *J. Chem. Soc., Dalton Trans.,* **1997**, 1.
7. Mingos, D.; Wales, D. *Introduction to Cluster Chemistry.* Prentice Hall: New Jersey, **1990**, pg. 3.
8. Churchill, M. R.; DeBoer, B. G. *Inorg. Chem.,* **1977**, 16, 878.
9. Drake, S. R.; Loveday, P. A. *Inorganic Synthesis, Vol. 28*, Angelici, R. J. Ed. Wiley: New York, **1990**, pg. 30.
10. Johnson, B. F. G.; Lewis, J.; Pippard, D. *J. Chem. Soc., Dalton Trans.*, **1981**, 407.
11. Clucas, J. A.; Foster, D. F.; Harding, M. M.; Smith, A. K. *J. Chem. Soc., Chem Comm.,* **1984**, 949.
12. Poe, A.; Sekhar, V. C. *J. Am. Chem. Soc.,* **1984**, 5034.
13. Deeming, A.; Donovan-Mtunzi, S.; Kabir, S. *J. Organometallic Chem.,* **1984**, 276, 3, c65.
14. Cartwright, S.; Clucas, J. A.; Dawson, R. H.; Foster, D. F.; Harding, M. M.; Smith, A. K. *J. Organometallic Chem.*, **1986**, 302, 3, 403.
15. Deeming, A.; Donovan-Mtunzi, S.; Kabir, S. *J. Organometallic Chem.,* **1987,** 333, 253.
16. Deeming, A.; Kabir, S. *J. Organometallic Chem.,* **1988**, 340, 3, 359.
17. Deeming, A.; Hardcastle, K.; Kabir, S. *J. Chem. Soc., Dalton Trans.,* **1988**, 827.

18. Kabir, S. E.; Miah, A.; Nesa, L.; Uddin, K.; Hardcastle, K. I.; Rosenberg, E.; Deeming, A. J. *J. Organometallic Chem.,* **1995**, 492, 41.

19. Bradford, C.W.; van Bronswijk, W.; Clark, R. J. H.; Nyholm, R. S. *J. Chem. Soc., Inorg. Phys. Theor.,* **1970**, 2889.

20. a) Benninghoven, A.; Rudenauer, F. G.; Werner, H. W. *Secondary Ion Mass Spectrometry: Basic Concepts, Instrumental Aspects, and Applications and Trends.* New York: Wiley, **1987**. b) Christie, W. H. *Anal. Chem.* **1981**, 53, 1240A.

21. Bruce, M. I.; Liddell, M. J. *J. Organometallic Chem.,* **1988**, 347, 157.

22. Yeh, W.; Li, C.; Peng, S.; Lee, G. *J. Organometallic Chem.,* **2004**, 689, 105.

23. Tseng, T. W.; Chen, M. C.; Keng, R. S.; Lin, Y. C.; Lee, G. H.; Wang, Yu. *J. Chinese Chem. Soc.,* **1991**, 38(6), 581.

24. Adams, R. D.; Horvath, I. T.; Wang, S. *Inorg. Chem.,* **1985**, 24, 1728.

25. Adams, R. D. *Metal-Ligand and Related Vibrations,* St. Martin's: New York, **1968**, pg. 98-101.

26. Davis, H. B. *Organometallics,* **1989**, 8, 1030-1039.

27. Beckett, M. A. *J. Organometallic Chem.,* **2003**, 688, 174 and references therein.

28. Jolly, P. W.; Stone, F. G. A. *J. Chem. Soc.,* **1965**, 5259.

29. Reimann, R. H.; Singleton, E. *J. Organometallic Chem.,* **1973**, 59, 309.

30. Cotton, F. A. *Chemical Applications of Group Theory*, New York: Wiley, **1990**.

31. Bond, A. M. *Inorg. Chem.,* **1977**, 16, 155.

32. Schmidt, S. P.; Trogler, W. C. *Inorganic Synthesis, Vol. 28*, Angelici, R. J. Ed. Wiley: New York, **1990**, pg. 162.

APPENDIX

Table A.1. Crystal Data and Structural Refinement Parameters

	$Os_3(CO)_{11}PPh_2(CH_2)_2PPh_2$	$Os_3(CO)_{11}PPh_2(CH_2)_2PPh_2Os_3(CO)_{11}$	$Os_3(CO)_{11}PPh_2(CH_2)_4PPh_2Os_3(CO)_{11}$	$Os_3(CO)_{11}PPh_2(CH_2)_2PPh_2W(CO)_5$
Empirical Formula	$C_{37}H_{24}O_{11}Os_3P_2$	$C_{48}H_{24}O_{22}Os_6P_2$	$C_{50}H_{28}O_{22}Os_6P_2$	$C_{42}H_{24}O_{16}Os_3P_2W$
Formula Weight	1277.10	2155.81	2183.86	1601.00
Temp. (K)	295(2)	296(2)	297(2)	296(2)
Crystal System, space group	Monoclinic, P2(1)/c	Triclinic, P -1	Monoclinic, C2/c	Monoclinic, P2(1)/n
a. (Å)	10.6539(3)	9.2108(6)	19.9931(5)	17.5204(4)
b. (Å)	16.8415(5)	10.0740(6)	17.2542(6)	13.4575(3)
c. (Å)	21.6729(4)	30.463(2)	17.8523(5)	19.6191(5)
α (°)	90	97.053(3)	90	90
β (°)	99.743(2)	95.705(3)	111.911(2)	92.9490(10)
γ (°)	90	96.985(3)	90	90
Volume ($Å^3$)	3832.63(17)	2765.6(3)	5713.6(3)	4619.68(19)
Z, D_{calc} (Mg/m^3)	4, 2.213	2, 2.589	4, 2.539	4, 2.302
Absorption coefficient (mm^{-1})	10.063	13.863	13.423	10.844
Crystal Size (mm)	0.35 x 0.28 x 0.15	0.30 x 0.28 x 0.03	0.28 x 0.22 x 0.03	0.31 x 0.14 x 0.04
θ_{max} (°)	25.03	23.26	25.02	23.26

Reflections collected, unique	40647, 6760	23050, 6916	26521, 5049	47770, 6619
R_{int}	0.0920	0.1300	0.100	0.077
Final R indices[I>2sσ(I)], R_1, wR_2	0.0375, 0.0748	0.1120, 0.3099	0.0623, 0.1494	0.0696, 0.1791
R indices (all data) R_1, wR_2	0.0693, 0.0832	0.2488, 0.3823	0.0850, 0.1637	0.0985, 0.2003
Largest diff. peak and hole (e.Å^{-3})	0.969 and -1.335	2.460 and -2.248	1.908 and -4.495	6.965 and -6.069

Figure A.1. IR Spectrum of $Os_3(CO)_{11}PPh_2(CH_2)_2PPh_2$ (hexanes solution)

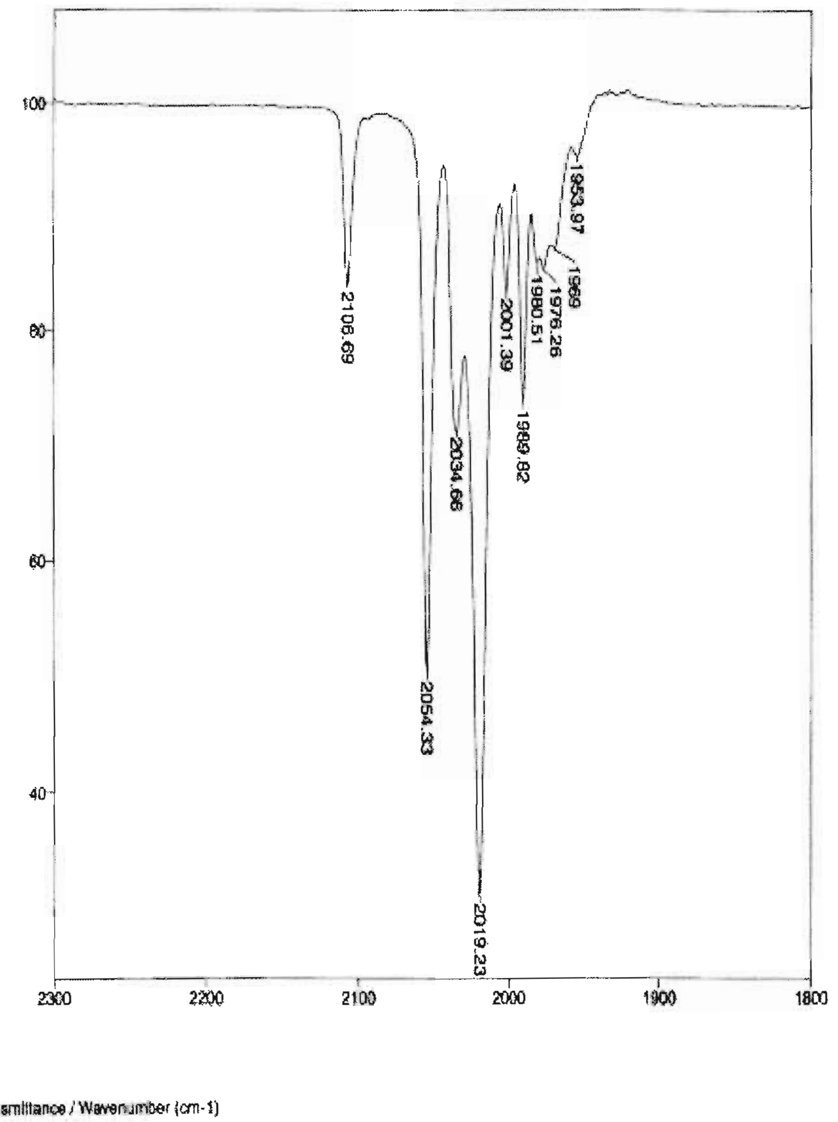

Figure A.2. IR Spectrum of $[Os_3(CO)_{10}PPh_2(CH_2)_4PPh_2]_2$ (hexanes solution)

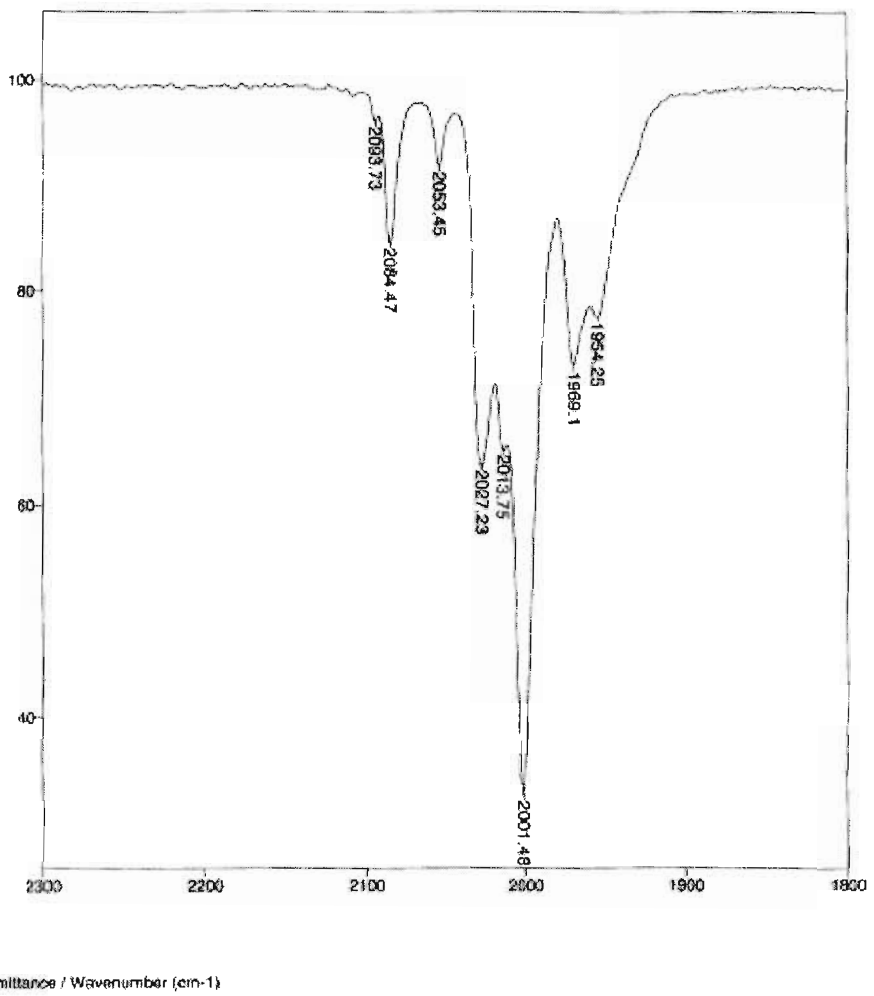

Figure A.3. IR Spectrum of $Os_3(CO)_{11}PPh_2(CH_2)_2PPh_2Re(CO)_4Br$ (hexanes solution)

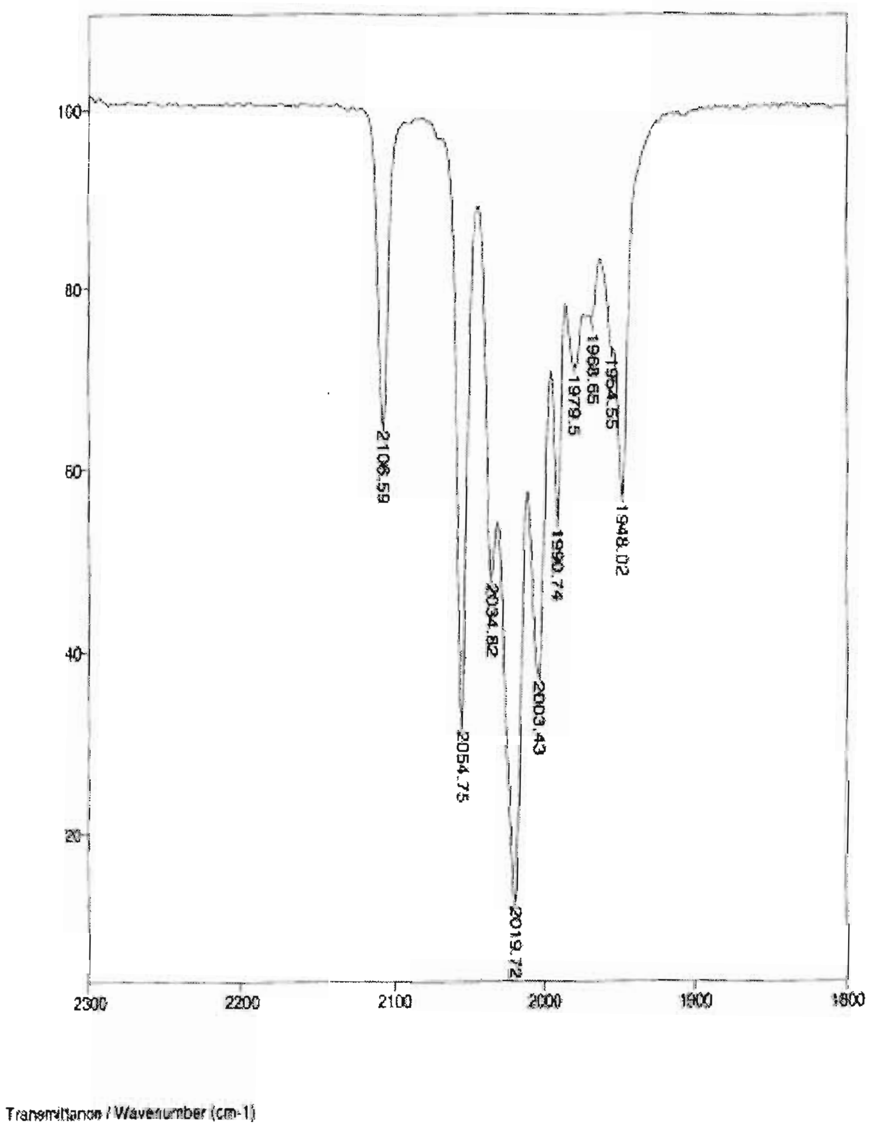

Figure A.4. IR Spectrum of $[Os_3(CO)_{11}PPh_2(CH_2)_nPPh_2]_2Re(CO)_3Br$ (hexanes solution)